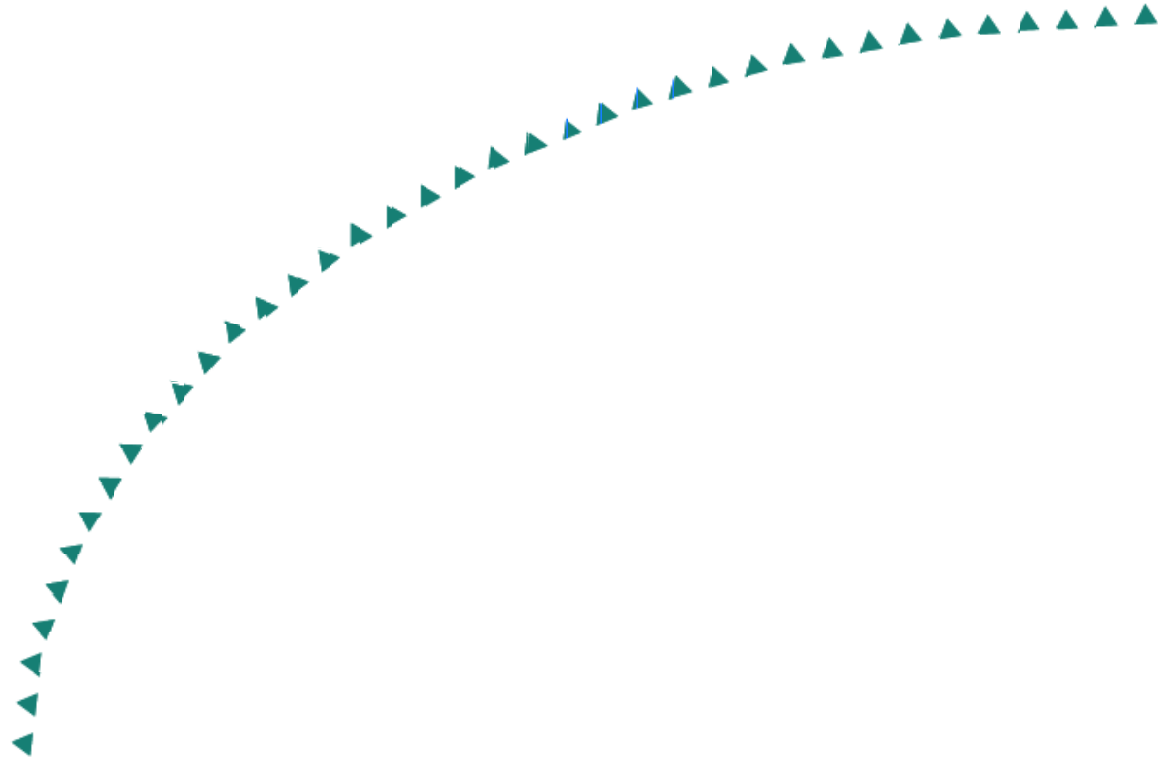


2004-17A

Final Report

**PERFORMANCE TESTING OF
EXPERIMENTAL
DOWEL BAR RETROFIT DESIGNS
PART 1 – INITIAL TESTING**



Technical Report Documentation Page

1. Report No. MN/RC- 2004-17A	2.	3. Recipients Accession No.	
4. Title and Subtitle PERFORMANCE TESTING OF EXPERIMENTAL DOWEL BAR RETROFIT DESIGNS PART 1 – INITIAL TESTING		5. Report Date December 2003	6.
7. Author(s) Trevor R Odden Mark B. Snyder Arturo E. Schultz		8. Performing Organization Report No.	
9. Performing Organization Name and Address University of Minnesota Department of Civil Engineering 500 Pillsbury Dr., S.E. Minneapolis, MN 55455-0116		10. Project/Task/Work Unit No.	
		11. Contract (C) or Grant (G) No. (c) 74708 (wc) 131	
12. Sponsoring Organization Name and Address Minnesota Department of Transportation 395 John Ireland Boulevard Mail Stop 330 St. Paul, Minnesota 55155		13. Type of Report and Period Covered Final Report	
		14. Sponsoring Agency Code	
15. Supplementary Notes www.lrrb.org/PDF/200417A.pdf			
16. Abstract (Limit: 200 words)			
<p>An area of concern common to portland cement concrete (PCC) pavements is load transfer across joints and cracks. The current design standard for load transfer in new jointed PCC pavements and the rehabilitation of old PCC pavement is to place steel dowel bars at mid-depth of the pavement across the joint or crack (1). The main issues with the use of retrofit and/or new dowels are the high expense associated with the retrofitting operation and the corrosion that has been associated with the use of steel dowels. Three new and experimental dowel bar retrofit designs, that address the issues of high retrofit cost and corrosion susceptibility, were tested in an accelerated manner in order to determine the potential viability of their use for the restoration of load transfer in PCC pavements. Innovations in the three designs included the use of fiber reinforced polymer dowels, grouted stainless steel pipe dowels, and a change in the geometric configuration of the design. An evaluation of test results and recommendations, regarding the use of the designs for the restoration of load transfer in PCC pavements, are presented.</p>			
17. Document Analysis/Descriptors Accelerated load testing Deflections Fiber reinforced polymer Repeated loads		18. Availability Statement No restrictions. Document available from: National Technical Information Services, Springfield, Virginia 22161	
19. Security Class (this report) Unclassified	20. Security Class (this page) Unclassified	21. No. of Pages 69	22. Price

PERFORMANCE TESTING OF EXPERIMENTAL DOWEL BAR RETROFIT DESIGNS

PART 1 – INITIAL TESTING

Final Report

Prepared by:

Trevor D. Odden
Mark B. Snyder
Arturo E. Schultz
Department of Civil Engineering
University of Minnesota

December 2003

Published by:

Minnesota Department of Transportation
Office of Research Services
Mail Stop 330
Transportation Building
395 John Ireland Boulevard
St. Paul, Minnesota 55155-1899

This report represents the results of research conducted by the authors and does not necessarily represent the views or policies of the Minnesota Department of Transportation and/or the Center of Transportation Studies. This report does not contain a stand or specified technique

The authors and the Minnesota Department of Transportation and/or the Center of Transportation Studies do not endorse products or manufacturers. Trade or manufacturers' names appear herein solely because they are considered essential to this report.

Acknowledgements

This research would not have been possible without the generous support of the Minnesota Department of Transportation (Mn/DOT) and the Department of Civil Engineering of the University of Minnesota. In particular, the authors would like to thank Thomas Burnham and Rebecca Embacher – Mn/DOT Materials Laboratory, and Ann McClellan – Mn/DOT Office of Research and Strategic Services.

Table of Contents

	Page
1. INTRODUCTION.....	1
1.1 Problem Statement.....	1
1.2 Research Objective.....	1
1.3 Research Approach.....	1
1.4 Scope.....	2
2. LITERATURE REVIEW.....	3
2.1 Load Transfer.....	3
2.1.1 Introduction.....	3
2.1.2 Locations Requiring Load Transfer.....	3
2.1.3 Measuring Load Transfer.....	3
2.2 Load Transfer Devices.....	5
2.2.1 Introduction.....	5
2.2.2 Aggregate Interlock.....	5
2.2.3 Mechanical Load Transfer Devices.....	6
2.3 Dowel Bars.....	8
2.3.1 Introduction.....	8
2.3.2 Installation of Dowel Bars.....	9
2.3.3 Problems Associated with Dowel Bars.....	11
2.3.4 Research on the Use of Non-Corrosive Dowel Bars.....	11
3. DESCRIPTION OF MINNE-ALF TEST PLATFORM AND CURRENT TEST PROGRAM.....	13
3.1 Development of the Minne-ALF.....	13
3.2 Current Minne-ALF Test Setup.....	18
3.2.1 Capabilities of the Current Minne-ALF Test Setup.....	18
3.2.2 Description of Test Stand and Hydraulic System.....	20
3.2.3 Description of Test Control and Data Acquisition Systems.....	20
3.3 Verification of Minne-ALF Test Program.....	21
3.3.1 Introduction.....	21
3.3.2 Description of Testing and Test Specimens.....	22
3.3.3 Results.....	23
4. DESCRIPTION OF RESEARCH PROGRAM AND TEST PROCEDURE.....	24
4.1 Introduction.....	24
4.2 Test Variables.....	24
4.3 Measures of Comparison.....	24
4.3.1 Introduction.....	24
4.3.2 LTE.....	24
4.3.3 Differential Deflection.....	24

4.3.4 Observed Behavior	24
4.4 Description of Test Specimens	25
4.4.1 Test Foundation	25
4.4.2 Test Slabs	25
4.4.3 Dowel Bar Retrofit Designs	26
4.5 Description of Data Acquisition	27
4.6 Test Procedures	28
4.6.1 Preparation of Test Specimen	28
4.6.2 Assembly of Test System	30
4.6.3 Calibration of Test System and Pretest Procedures	31
5. RESULTS AND ANALYSIS	32
5.1 Data Analysis	32
5.2 Results	32
5.2.1 Influence of Changing Dowel Bar Material	32
5.2.2 Influence of Changing Dowel Bar Configuration	39
6. CONCLUSIONS AND RECOMMENDATIONS	40
6.1 Introduction	40
6.2 The Use of FRP Dowel Bars in Dowel Bar Retrofits	41
6.3 The Use of Grouted Stainless Steel Dowel Bars in Dowel Bar Retrofits	41
6.4 The Use of Shallow Cover Retrofit Dowel Bars	42
REFERENCES	43
APPENDIX A: Minne-ALF Test Frame Drawings	45
APPENDIX B: Minne-ALF Demonstration Testing Results	54

List of Tables

Table 3-1: Summary of Minne-ALF Design Requirements	14
Table 3-2: Desired and Existing Minne-ALF Capabilities	19
Table 4-1: Summary of Test Slab Compressive Strengths	25
Table 4-2: Summary of Test Slab Static Moduli of Elasticity	26
Table 4-3: Summary of Compressive Strength of Backfill Material	27
Table 4-4: Initial LVDT Positions	28
Table 5-1: Summary of Test Results	33
Table 5-2: Physical Properties of Dowel Bars	37

List of Figures

Figure 2-1: Photograph of a Dynatest Falling Weight Deflectometer	5
Figure 2-2: Mechanical Drawing of Double-Vee Shear Load Transfer Device	7
Figure 2-3: Studded Plate Load Transfer Device	8
Figure 2-4: Typical Dowel Bar Retrofit Design	10
Figure 3-1: Transverse Elevation of Original Minne-ALF Test Stand Design	16
Figure 3-2: Longitudinal Elevation of Original Minne-ALF Test Stand Design	17
Figure 3-3: Plot of Command Wave Forms	21
Figure 4-1: Photograph of LVDT's	27
Figure 4-2: Photograph of Slot Preparation	29
Figure 4-3: Photograph of Dowel Bars and Slots Prior to Retrofitting	30
Figure 4-4: Photograph of Mine-ALF Prior to Test	31
Figure 5-1: Influence of Changing Dowel Bar Material on Load Transfer Efficiency	34
Figure 5-2: Influence of Changing Dowel Bar Material on Differential Deflection	34
Figure 5-3: Pressure Exerted on Loaded Dowel	36
Figure 5-4: LTE Histories for Slabs 1 and 3 for Equal Testing Periods	38
Figure 5-5: Influence of Changing Dowel Bar Configuration on Load Transfer Efficiency	39
Figure 5-6: Effect of Various Dowel Bar Configurations on Differential Deflection	40
Figure A-1: Base Plan View	46
Figure A-2: Base Longitudinal View with Details	47
Figure A-3: Longitudinal Elevation of Minne-ALF	48

Figure A-4: Longitudinal Elevation of Minne-ALF Showing Knee Brace.....	49
Figure A-5: Minne-ALF Transverse Elevation.....	50
Figure A-6: Cutaway of Minne-ALF Transverse Elevation Showing Rocker Beam Configuration.....	51
Figure A-7: Two-Pin Hinge Connection between Rocker Beam and Frame.....	52
Figure A-8: Rocker Beam.....	53
Figure B-1: Effect of Joint Face Texture on Load Transfer Efficiency.....	55
Figure B-2: Effect of Joint Face Texture on Differential Deflection.....	55
Figure B-3: Effect of Concrete Backfill Material on Load Transfer Efficiency.....	56
Figure B-4: Effect of Concrete Backfill Material on Differential Deflection.....	56
Figure B-5: Effect of Dowel Bar Length on Load Transfer Efficiency.....	57
Figure B-6: Effect of Dowel Bar Length on Differential Deflection.....	57
Figure B-7: Effect of Dowel Bar Type on Load Transfer Efficiency.....	58
Figure B-8: Effect of Dowel Bar Type on Differential Deflection.....	58

Executive Summary

Portland cement concrete (PCC) pavements are jointed, by nature of their construction. Moreover, exposure to changes in temperature and humidity, as well as axle loadings, often induces cracking. Thus, an area of concern regarding the management of PCC pavements is load transfer across joints and cracks. Improving load transfer in jointed and cracked pavements enhances riding quality, which offers benefits in terms of traffic flow, driver safety and vehicle wear.

The current design standard for load transfer in new jointed PCC pavements, and the rehabilitation of old PCC pavements, is to place steel dowel bars at mid-depth of the pavement across the joint or crack (1). The main issues with the use of retrofit and/or new dowels are the high expense associated with the retrofitting operation and the corrosion that has been associated with the use of steel dowels.

Three new and experimental dowel bar retrofit designs, that address the issues of high retrofit cost and corrosion susceptibility, were tested in an accelerated manner in order to determine the potential viability of their use for restoration of load transfer in PCC pavements. Innovations in the designs included the use of fiber reinforced polymer dowels, grouted stainless steel pipe dowels, and a change in the geometric configuration of the design. An evaluation of test results and recommendations, regarding the use of the designs for restoration of load transfer in PCC pavements, are presented.

The performance of the innovative dowel bar designs (Slabs 2, 3 and 4) is evaluated in comparison with that for the standard design (Slab 1), which featured 1.5-in. diameter epoxy-coated mild steel dowels with a 15-in. length, 3-in. clear cover and 12-in. spacing. Slab 1 demonstrated excellent performance in terms of large Load Transfer Efficiency (LTEs) (in excess of 90%) and small differential deflections (less than 2.5 mils) over the duration of the test (10.5 million cycles), which was continued beyond the standard duration of 6.7 million cycles.

Test Slab 2, with fiber-reinforced polymer (FRP) dowels of the same size and configuration as the mild steel dowels used in the standard detail (Slab 1), exhibited the poorest performance in terms of smaller LTEs and larger differential deflections. However, the measured values for these parameters at the end of the test (6.7 million cycles) were still superior to the accepted limits (LTE > 70% and diff. deflect. < 5 mils). It is suggested that a larger diameter FRP dowel, in which the increase in diameter is used to compensate for the lower modulus of elasticity of the FRP material, may offer comparable performance to the standard dowel bar retrofit detail.

Test Slab 3, with grouted, stainless steel dowel bars (1.66-in. diameter, 1/8-in. wall thickness, 18-in. length, 3-in. clear cover and 12-in. spacing), performed as well as Slab 1 during the first 10.5 million cycles of loading. This test was extended beyond the standard duration to 13.5 million cycles. Measurements taken in the last 1.5 million cycles of this extended duration exhibited rapid deterioration of performance, with LTEs that meet acceptable performance (LTE > 70%) but with differential deflections approaching the 5 mil limit.

Test Slab 4, which was nominally identical to Slab 1 except that clear cover was reduced from 3 in. to 2 in., performed as well as Slab 1. This test was continued beyond the standard duration of

6.7 million cycles to 12.4 million cycles. The reduction in clear cover does not appear to have affected load transfer at the joint.

1. INTRODUCTION

1.1 Problem Statement

In today's society, there is an increasing demand for high performance, economical, and long lasting highway pavements. This increasing demand has been brought into existence by the public's intolerance of transportation delays and our fast paced economy. In order to improve on current highway pavements, research must be conducted on new and experimental designs that address the deficiencies in current pavement designs and rehabilitation techniques.

One such area of concern common to portland cement concrete (PCC) pavements is load transfer across joints and cracks. Load transfer is the transmission of load or stress from a loaded slab to adjacent slabs and is accomplished through grain or aggregate interlock, or the use of mechanical devices. Many types of mechanical devices are used for load transfer, including dowel bars, studded plates, and tie bars. The underlying function of all load transfer devices is to provide vertical shear transfer across a slab crack or joint, thereby reducing the stresses and deflections in the loaded slab. Load transfer devices placed across expansion and contraction joints are required to transfer shear while allowing horizontal movement (expansion and contraction) of the joint. In these cases, the use of aggregate interlock and tie bars can be problematic. In the aggregate interlock load transfer mechanism, opening of the joint leads to a reduction of the interlock between the faces of the joint thereby decreasing the ability to transfer shear. Tie bars on the other hand, maintain shear transfer capacity but don't allow the joint to expand or contract. The current design standard for load transfer in new PCC pavements, and the rehabilitation of old PCC pavements, is to place steel dowel bars at mid-depth of the pavement across the joint or crack (1).

The main issues of concern with the use of retrofit and/or new dowels are the high expense associated with the retrofitting operation and the corrosion that has been associated with the use of steel dowels. This corrosion is detrimental to the structural integrity of the joint, causing an increase in the volume of the dowel bar that can "lock" the joint, preventing it from expanding and contracting. This prohibits the relief of the slab stresses caused by temperature and moisture gradients in the concrete. Consequently, mid-panel tension cracks may form or spalling may occur near joints and/or cracks. This results in an overall decrease in the quality of the riding surface of the pavement and leads to a reduction of traffic flow, increased danger to drivers and increased wear on vehicles.

1.2 Research Objective

The objective of this research project was to test new and experimental dowel bar retrofit designs in an accelerated manner in order to determine the potential viability of their use for the restoration of load transfer in PCC pavements. The designs that were tested address the previously stated issues of high retrofit cost and corrosion susceptibility. The use of accelerated testing was extremely important to this research because the collection of suitable long-term field data can take many years to acquire, resulting in delays in the implementation of new and potentially more effective designs.

1.3 Research Approach

The approach taken to achieve the stated objectives can be summarized in the following steps, which define the laboratory test and verification program:

1. Determine possible dowel bar retrofit designs that address the issues of high retrofit cost and/or corrosion susceptibility.
2. Establish criteria for comparing the performance of the potential designs with a standard design.
3. Test both the potential and the standard dowel bar retrofit designs using the Minnesota Accelerated Load Facility (Minne-ALF) test program. A history and background of this test program is given in Chapter 3. A full description of the test program and procedures is provided in Chapter 4. Additional information can be found in technical references (2, 3, and 4).
4. Using the established criteria, determine the relative performance of the different designs and compare the results.
5. Formulate conclusions and recommendations based on the comparison of the test results.

The specific details of this research approach are documented in subsequent chapters of this report. Chapter 2 contains a literature review that addresses load transfer in PCC pavements, devices for improved load transfer, and a detailed description of the dowel bar detail. Chapter 3 describes the Minne-ALF test platform for accelerated load testing of pavements. Chapter 4 is a description of the current testing program on dowel bar retrofit designs for restoring load transfer in PCC pavements. Chapter 5 presents the test data and offers an analysis of the performance of the test slabs. Chapter 6 summarizes the report and provides pertinent conclusions.

1.4 Scope

The scope of this research is limited to the evaluation of four dowel bar retrofit designs tested using the Minne-ALF test program. This includes the accompanying material testing, data analysis, and test procedures involved with the test program. The designs that were included address the previously stated issues of high retrofit cost and corrosion susceptibility. The specific designs tested were selected on the basis of probable cost effectiveness by a selected group of research engineers from the University of Minnesota and the Minnesota Department of Transportation.

2. LITERATURE REVIEW

2.1 Load Transfer

2.1.1 *Introduction*

Load transfer is the transfer of load or stress from a loaded slab to adjacent slabs through grain or aggregate interlock, or the use of mechanical devices. Inadequate load transfer results in high stresses in the loaded slab and large deflections relative to the adjacent slabs. These conditions may result in pumping and faulting, cracking, and/or spalling of the slab.

Pumping is the mechanism through which water and foundation materials are transported and deposited at other locations beneath the slab or are forced up through joints or cracks onto the surface of the pavement. This mechanism is produced when there is high relative vertical movement (or deflection) between adjacent slabs as the load moves across the crack or joint and in the presence of free water and erodible foundation materials. Pumping erodes support material beneath the slab and leads to nonuniform slab support conditions. Subsequently, faulting or cracking usually follows due to loading of the slab and the given support conditions.

Cracking and spalling are often the result of the high load-related stress concentrations that develop near the slab corners or edges due to the reduced area of concrete resisting the applied load in these regions. Spalling is common on both the top and bottom surfaces of the slab along the joint edges; where relatively large vertical movements occur, which cause binding of the slabs.

2.1.2 *Locations Requiring Load Transfer*

In order to maintain a high quality pavement, adequate load transfer must be provided at any discontinuity in the pavement. These discontinuities include full-depth cracks, contraction joints, expansion joints, and construction joints. Full-depth cracks can form randomly across pavements. They are caused by high stresses from mechanical loads and temperature and moisture gradients. Cracks typically form in planes of weak concrete. Contraction joints are usually formed during construction or cut shortly after construction. The main purpose of contraction joints is to control the position of cracking caused by shrinkage and temperature stresses. Expansion joints are used in pavements to prevent the formation of high compressive stresses, by providing a small gap for the concrete to expand. Typically, they are located where the pavement meets another structure, such as a building or a manhole cover. Construction joints are necessary to allow for the proper construction of the pavement. An example of a common construction joint is the joint formed at the end of a day of paving. This type of joint is usually formed and is smooth requiring either mechanical load transfer devices or shear keys. It is essential that load transfer is maintained across all types of joints or full-depth cracks in order avoid deterioration of the pavement by means of the distress discussed in the preceding section.

2.1.3 *Measuring Load Transfer*

Load Transfer is measured by means of a parameter known as the load transfer efficiency (LTE), which is defined as “the ability of a joint or crack to transfer load from one side of the joint or crack to the other.”(1) The following three equations are the most commonly used formulas for determining LTE, and equation 2-1 is the most widely accepted and used of the three equations (1):

$$LTE = \frac{\Delta_{UL}}{\Delta_L} \times 100 \quad (2-1)$$

$$LTE = \frac{2\Delta_{UL}}{\Delta_L + \Delta_{UL}} \times 100 \quad (2-2)$$

$$LTE = \frac{\sigma_{UL}}{\sigma_L} \times 100 \quad (2-3)$$

where:

Δ_{UL} = the deflection of the unloaded slab;

Δ_L = the deflection of loaded slab;

σ_{UL} = the stress in unloaded slab; and

σ_L = the stress in loaded slab.

In the deflection LTE formulas (equations (2-1) and (2-2)), when the deflection of the loaded side of a crack or joint is equal to the deflection of the unloaded side, there is 100 percent LTE. If the unloaded side of the crack or joint does not deflect when the other side is loaded, there is zero percent LTE. This is similar for the stress LTE equation, but using respective stresses in the loaded and unloaded slabs. The stress and deflection LTE equations are not directly proportional, but are a function of the slab properties (1). A LTE value of 70 to 100 percent is typically regarded as adequate, while LTE values lower than 50 percent are typically associated with the previously described distresses that cause pavement deterioration (15).

In order to compute LTE, the deflections on both sides of the crack or joint must be determined. A device known as a falling weight deflectometer (FWD) is usually used to determine these deflections. The falling weight of this device is used to simulate the impulse load of a heavy vehicle moving across the pavement. Figure 2-1 is an illustration of a typical FWD.

The FWD drops a mass package onto a load plate which has been positioned on one side of the crack or joint. At the center of the load plate and at varying distances from the crack or joint on the unloaded slab are sensors that record the response of the pavement to the impulse load. From these readings, deflections are computed and the LTE is determined using the readings from the plate sensor and the first sensor on the other side of the joint or crack, which is located within 6 inches of the joint or crack. It is important to note that deflection testing should be conducted at temperatures below 80 degrees to avoid seeing artificially high LTE values caused by expansion of the slabs and subsequent locking of the joints. Testing at temperatures below 80 degrees will produce more accurate LTE values and can more accurately indicate if there is a potential load transfer problem.

Another important factor that is used to determine adequate load transfer is differential deflection. Differential deflection (DD) is the relative displacement between the loaded and unloaded sides of the joint or crack. It is computed by taking the difference of the displacements, as illustrated in equation 2-4.

$$DD = \Delta_L - \Delta_{UL} \quad (2-4)$$



Figure 2-1 Photograph of a Dynatest Falling Weight Deflectometer

Differential Deflection is frequently used to provide additional information about the performance of the joint or crack. This is best illustrated in an example of a deflection test of two different joints taken from technical literature (4).

The first joint, may have $\Delta_L = 0.02$ in. and $\Delta_{UL} = 0.01$ in., while the second joint may have $\Delta_L = 0.008$ in. and $\Delta_{UL} = 0.004$ in. Both joints would have the same LTE of 50 percent, but the first joint would clearly be of greater concern because the higher differential deflections would be more likely to produce pumping, faulting and spalling.

2.2 Load Transfer Devices

2.2.1 *Introduction*

Load transfer devices are used to provide adequate load transfer across discontinuities in the pavement. There are two major categories of load transfer devices: aggregate interlock and mechanical devices. The underlying function of all load transfer devices is to provide vertical shear transfer across the crack or joint in the slab. This reduces the stresses in the loaded slab by providing a larger area to resist the applied load. In most cases, load transfer devices are required to perform while allowing horizontal movement caused by expansion and contraction of the pavement. In these cases, the use of certain load transfer devices can be problematic.

Aggregate Interlock

Aggregate interlock is a load transfer mechanism that is developed through friction and interlock of the two faces of the fracture plane in the concrete slab at the location of the joint or crack. This interlock is dependent on the joint/crack width, as the temperature decreases the gap increases reducing interlock and thereby decreasing the ability to transfer load. Hard irregular or

crushed aggregates can provide good interlock. Gravel or easily polished aggregates tend to provide a lower amount of aggregate interlock due to their low friction coefficients.

Aggregate interlock can be an effective way to provide load transfer, provided the joint or crack remains tight. However, aggregate interlock cannot be typically counted on for load transfer, due to the unreliability of the mechanism. If temperature fluctuations or pavement shrinkage cause the joint or crack to open, interlock is greatly reduced or eliminated. Consequently, load transfer by aggregate interlock is greatly reduced.

2.2.3 Mechanical Load Transfer Devices

Many types of mechanical devices have been used for load transfer, including dowel bars, tie bars, double-vee shear devices and studded plates, to name a few. The concept of mechanical load transfer devices is to physically attach the two sides of the crack or joint. This causes the two sides of the discontinuity to act together and resist differential deflection, allowing shear loads to be effectively transferred across the joint or crack. Dowel bars are the standard mechanical load transfer devices used in pavements today due to their reliability and established field performance. This type of mechanical load transfer device is described in detail in the next section of this chapter.

Tie bars are pieces of standard deformed reinforcing bar. Typically, they are used in longitudinal joints where slabs can be rigidly attached or “tied” together. In these joints, horizontal movement can be restrained due to the short widths of the pavement and the low expansion and contraction stresses in the transverse direction. Tie bars are typically not used in transverse joints, because they restrict the horizontal movement of the slabs. Tie bars are made in standard reinforcing bar sizes and grades, typically they are #4 or #5 bars. Often, a corrosion resistant coating, such as epoxy, is applied to resist environmental conditions and deicing salts. Installation of tie bars is generally performed at the time of pavement construction, but they can also be retrofitted in certain types of repairs such as lane additions.

Another mechanical load transfer device is the double-vee shear device. This type of device is used to restore load transfer and requires retrofitting in an existing pavement. Figure 2-2 (1) illustrates this device. The double-vee device is made of two steel v-shaped sections. The outsides of the steel sections are padded with foam that allow for joint movement. The center of the device is also filled with foam to keep the joint clean and free of incompressible materials. The device is compressed and installed in a cored hole in the concrete pavement at the joint or crack. The precompression reduces the stresses in the repair as the joint expands. Some research has shown that the use of these devices are less effective in restoring load transfer than other mechanical load transfer devices (5).

Studded plates have also been used to restore load transfer across joints or cracks. Figure 2-3 (1) illustrates this type of device. They are made of two steel plates connected by a steel stud that extends through the plates. The device is installed by epoxying it in a cored hole at the joint or crack. This type of load transfer device is not widely used and little information is available regarding its performance.

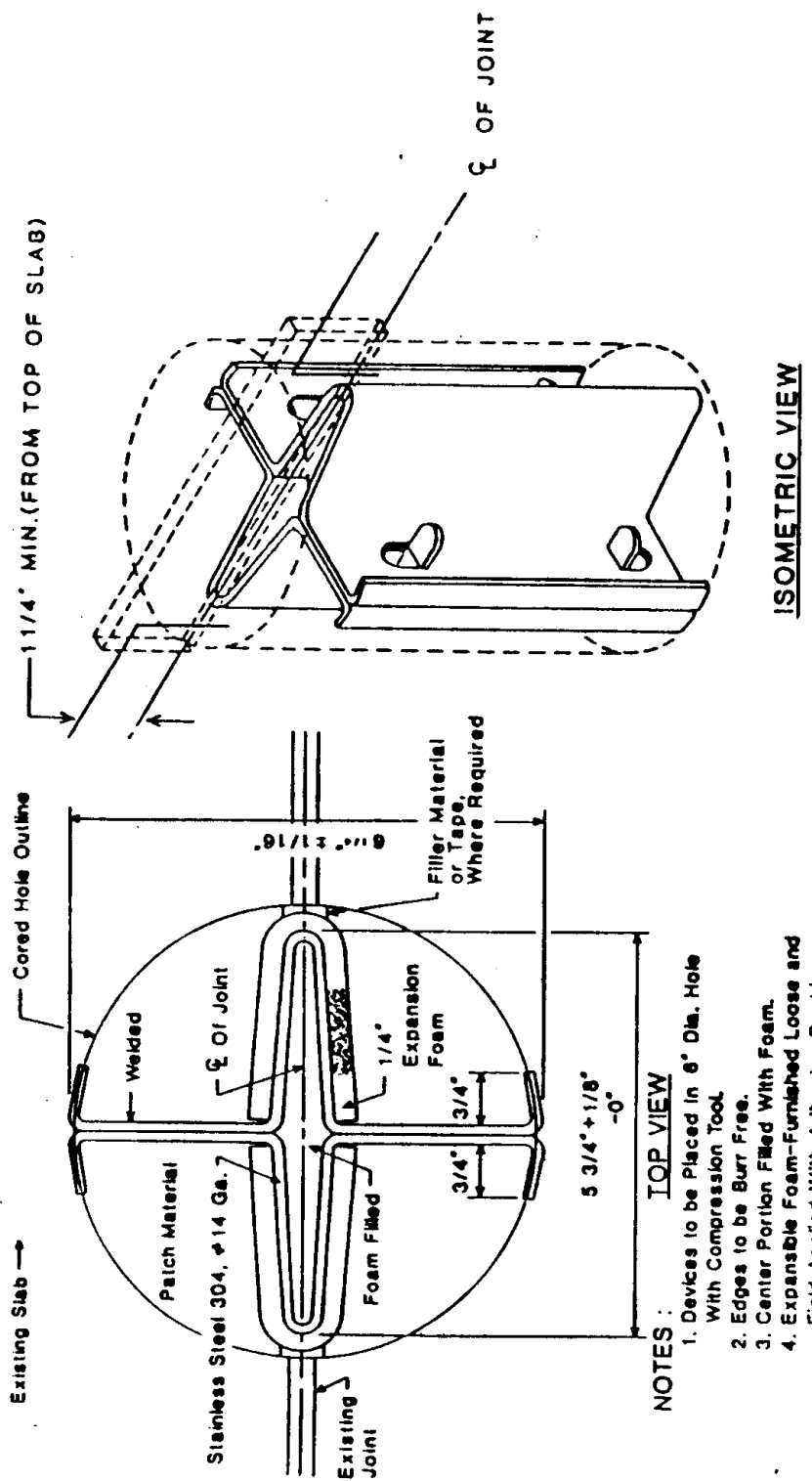


Figure 2-2 Mechanical Drawing of Double-Vee Shear Load Transfer Device (1)

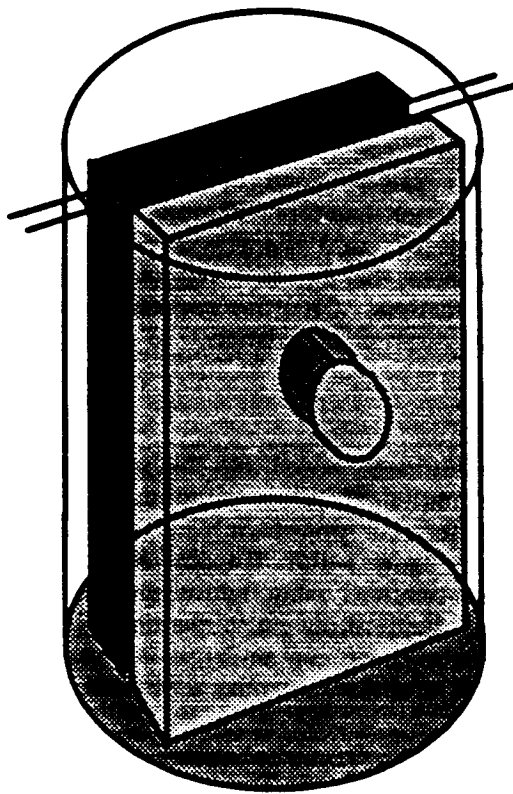


Figure 2-3 Studded Plate Load Transfer Device (1)

2.3 Dowel Bars

2.3.1 Introduction

Dowel bars are the standard for mechanical load transfer devices used in PCC pavements today. They provide vertical shear reinforcement while allowing for expansion and contraction of the joint or crack. They are smooth bars that are placed across the pavement discontinuity, parallel to the major axis of the roadway. Dowel bars come in a variety of shapes, sizes, and materials. The standard dowel bar design uses round, mild steel bars, with a diameter equal to approximately 1/8 the thickness of the slab (i.e. 1-inch diameter bar in an 8-inch thick slab). Dowel bars are typically 18 inches in length, but some states including Minnesota use bars 14 to 16 inches long. The spacing and size of the dowel bars depends on the applied loads and the thickness of the pavement. The closer the spacing and the larger the diameter of the dowels, the larger the bearing area will be, thus reducing the bearing stresses caused by vehicle loads. Dowel bars are often coated with a corrosion resistant material, such as epoxy. They are usually placed at the mid-depth of the slab and are spaced approximately twelve inches apart. Although round dowels are the most widely used, a bar with I-beam cross section has been used in some projects (1) and research is now being conducted on different shaped dowels, including flat plates and oval dowel bars, that increase the bearing area without increasing the cost or mass the dowel bar. Dowel bars are generally made of mild steel, but research is now being performed on other types of materials including: fiber reinforced plastic (FRP), solid stainless steel, stainless steel clad, and grouted, stainless steel pipe to name a few.

2.3.2 Installation of Dowel Bars

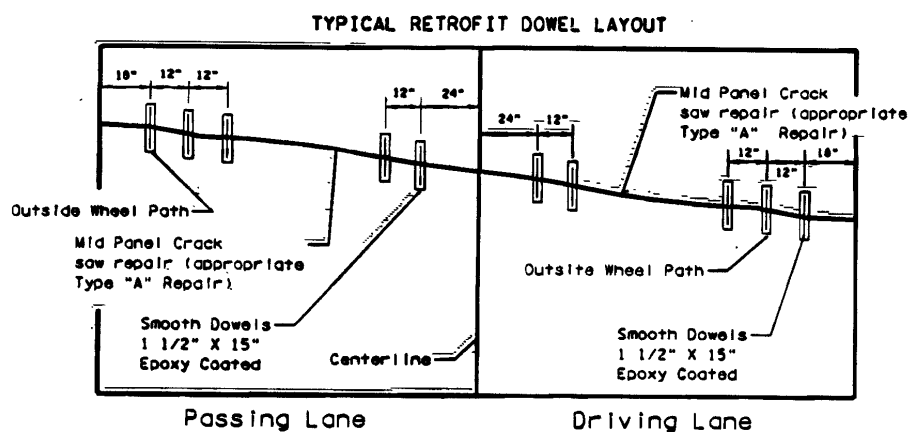
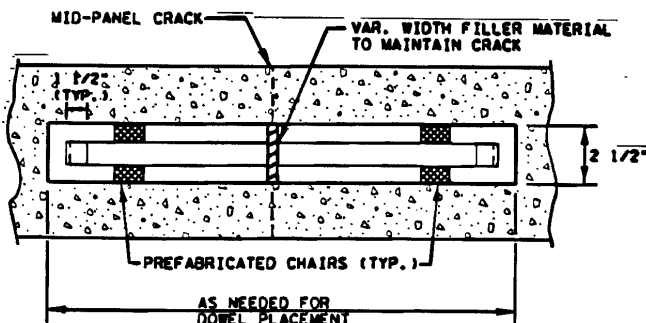
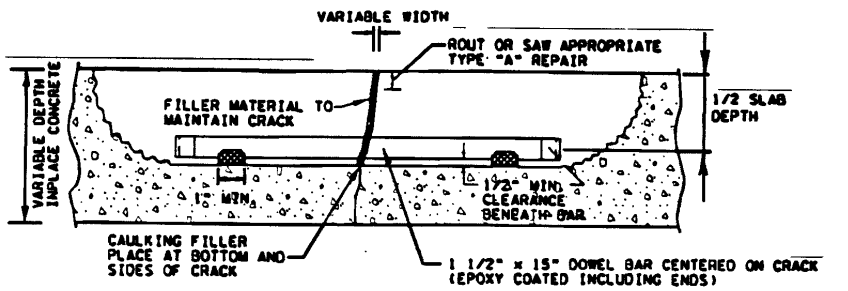
Dowel bars are used in both new construction and in the rehabilitation of old pavements. In new jointed concrete pavement construction, dowel bars are placed across the width of the pavement at the locations of the transverse joints, typically 12 to 20 feet apart in the longitudinal direction (1). They are tack-welded into steel wire cages known as “baskets.” The transverse spacing between dowels is typically twelve inches. The use of dowel baskets allows for the correct placement and alignment of the dowel bars, both vertically and horizontally. This is critical for proper operation of the joint. If the dowel bars are placed askew, the joint may not be able expand and contract properly, prohibiting the relief of high tensile stresses caused by temperature and moisture changes in the concrete pavement, which can cause slab cracking. Prior to paving, the dowels are typically coated with a debonding agent or lightweight oil. This will allow the joint to expand and contract freely once the concrete has hardened. After the dowels have been properly placed and prepared, the paver places the concrete. The paver moves directly over the dowel baskets, encasing the dowel bars in concrete. After the concrete has hardened, the transverse joints are cut over the mid-point of the dowels. The cuts are generally made to a depth of $\frac{1}{4}$ the thickness of the slab creating a weakened plane in the concrete where contraction cracks propagate through the remaining thickness of the slab. The joints are then sealed to prevent the ingress of debris.

In rehabilitation projects, where load transfer restoration is required, dowel bars are retrofitted. Load transfer restoration is usually performed over large cracks, undoweled joints, or in joints where the dowel bars have failed. Figure 2-4 (7) illustrates a typical dowel bar retrofit design. The retrofit process entails cutting and chipping slots across the joint or crack. Each slot is formed by making two or more saw cuts parallel to the flow of traffic at the desired locations along the joint or crack. The depth of the cuts should allow the dowel to be placed at mid depth of the slab, including a minimum 0.5 inch clearance below the dowel bar (7) to allow for proper consolidation of the backfill material. The required length of the cuts is dependent on the length of the dowel bars and depth of the cut, but is generally 2 to 3 feet long. The width of the slot varies, but is typically in the range of 2 to 4 inches. Once the cuts have been made, the slot material can be removed using a small chipping hammer or hand tools. The slot must be cleaned using a sandblaster in order to provide a good bonding surface for the backfill material (1). After the slot has been properly cleaned, a bonding agent is applied to the bottom and sides of the slot. Bonding agents range from simple mortars to epoxy resins. A piece of plywood or foam is wedged into the slot near the center of the dowel to prevent repair material from intruding into the existing joint and to allow reestablishment of the joint. End caps are also placed on the retrofit dowels to allow the joint to close without producing bearing stresses in the concrete at the ends of the dowel. End caps are not used in new construction because at the time of construction, prior to cutting the joints, is the tightest the joints will be.

Prior to installation, the retrofit dowel is coated with a light oil or debonding agent. It is then placed on chairs in the slot to maintain the half-inch clearance required for consolidation of the backfill material. Once the dowels are properly aligned, the slot can be backfilled. The backfill material should be low-shrinkage, to preserve the bond with the concrete slab. Care must be taken to provide good consolidation around the dowel bar. Following curing, the repair can be opened to traffic, diamond ground, and/or overlaid. LTE values of 90 to 100 percent should be expected in properly installed retrofit dowel bar installations (1).

DOWEL BAR RETROFIT

DESCRIPTION: THIS REPAIR IS INTENDED TO BE USED TO ESTABLISH/RESTORE LOAD TRANSFER AT JOINTS OR CRACKS.



- ① CONTACT THE CONCRETE ENGINEERING UNIT FOR SPECIAL PROVISIONS, MATERIALS, STANDARD PLATES, AND CONSTRUCTION DETAILS

DATE: January, 2000

Figure 2-4 Typical Dowel Bar Retrofit Design (7)

2.3.3 Problems Associated with Dowel Bars

Although dowel bars are currently the most effective means of providing load transfer, they are not free from problems. Issues of cost, corrosion and improper installation have been the largest sources of concern.

One of the principal concerns is the susceptibility to corrosion of the standard mild steel dowel bars. Mild steel dowels with an epoxy coating are not immune to this problem either (14). Epoxy coatings are easily nicked during construction or while in service, allowing for moisture and deicing salts to reach the steel. Corrosion then takes place causing an increase in the volume of the dowel bar. This increased volume tends to “lock” the joint, causing the slab movement stresses to be induced into the concrete. Often, tension cracks form or spalling occurs, reducing load transfer and initiating pavement deterioration.

Improper installation has a significant impact on sound performance of the joint. Dowel bars should be placed parallel to both the pavement surface and the major axis of the road way. Misalignment can also cause the joint to “lock” causing the expansion and contraction stresses to be induced into the concrete. This may result in tensile cracks and or spalling.

Research on The Use of Non -Corrosive Dowel Bars

Corrosion of dowel bars is not a new phenomenon. Solid stainless steel bars have been used in some projects, but due to their high cost, other types are now being investigated. The two common types of alternative dowel bars under consideration are fiber reinforced polymer (FRP) and grouted stainless steel pipe.

Rizkalla and Eddie (11, 12), at the University of Manitoba, have performed tests on glass fiber reinforced dowels (GFRP) and FRP dowels. Their test program consisted of three different series of tests, two static with varying support conditions and one cyclic. The test specimens consisted of three slabs; 10 inches thick, 2 feet wide, and 8 feet long. At the center of the slab, a 1/8-inch gap was formed to act as the joint for the first test series. In the second and third test series, half of the slab was cast with the other half being cast the next day against the initial slab, creating a smooth construction joint. Two 18-inch dowel bars were cast in place across the joint. Each test specimen contained a different type of dowel bar (1.5 inch diameter GFRP dowel, 1.5 inch diameter FRP dowel, or 1.25 inch epoxy coated steel dowel).

The first test series used steel springs to simulate a weak soil support condition. A load was applied to a plate on one side of the joint by a MTS hydraulic actuator. The load was slowly increased until “excessive” deflections occurred. Relative performance was measured in terms of differential deflection and LTE. Slab displacements were measured by linear variable displacement transducers (LVDT’s). For each test specimen, differential deflection and LTE were then computed and plotted on differential deflection versus load and LTE versus load graphs. The GFRP dowels performed the best, exhibiting the lowest differential deflection and highest LTE (for any given load), with the steel dowels following.

The second test series consisted of six test specimens (2 replicates of each type of dowel bar material) with a typical gravel base. A load was applied in a similar fashion to that used for the first test series. Differential deflection and LTE was again compared for each specimen. The

results were comparable with the first test series, with the GFRP dowels out-performing the steel and FRP dowels.

The third test series used a cyclically applied load on three different test specimens supported on the similar gravel base as in test two. Each test specimen was subjected to 1 million load cycles. The load was ramped from 4.5 kips to 29.2 kips in varying cycle increments. Both differential deflection and LTE were compared for each specimen, with the similar results as in the first two test series. The GFRP dowels out performing the steel and FRP dowels. The authors conclude that GFRP dowels outperformed the two other types of dowels tested. They believed the reason the GFRP dowels out performed the epoxy-coated steel dowels was due to their increased diameter. The researchers suggested that GFRP dowels could be a potential alternative to steel dowels, and they recommended further long-term testing of the GFRP dowels.

Black, Larson, and Stauton (6) performed a study on the use of stainless steel pipe and grouted stainless steel pipe as dowel bars. Their test program consisted of cyclically loading small concrete slab specimens containing two cast-in-place dowel bars. The slab contained a formed joint. A 1.25-inch diameter solid stainless steel dowel bar was used as a basis for comparison. Four other dowel bar materials were tested, they included; 1.66 inch diameter stainless steel pipe with a wall thickness of .065 inches, 1.66 inch diameter stainless steel pipe with a wall thickness of .109 inches, and grouted versions of the two types of pipe.

A load of 24 kips was applied cyclically for up to 100 cycles using a universal test machine. Relative performance of the test specimens was measured in terms of differential deflection. If the dowels had not failed after 100 cycles, the specimen was loaded until failure occurred. Deflections were measured using a dial gauge at 10-cycle intervals for all specimens and the values were compared. Both of the hollow pipe dowels failed during loading in the first cycle. The grouted pipe dowels and the solid stainless steel dowel endured all 100 test cycles and were subsequently loaded until failure. The 0.109 inch thick wall, grouted pipe performed the best with the thinner wall grouted pipe following. The solid stainless steel dowel was out performed by both types of grouted pipe dowels. The authors believed this was due to the increased bearing area and moment of inertia of the larger diameter grouted pipe dowels. They suggested that the use of the 1.66 inch diameter, 0.109 inch thick walled, grouted stainless steel pipe dowels to be a more cost effective and better performing alternative to standard steel dowels in PCC pavements with short joint spacings.

The Highway Innovative Technology Evaluation Center (HITEC) (13) is now performing a field study on the performance of both FRP and stainless steel dowels. There are five different field sites including: Illinois, Iowa, Kansas, Ohio and Wisconsin. The specific dowel bar materials being tested include: 18 inch long GFRP dowels with a minimum diameter of 1.5 inches, 18 inch T304 stainless steel solid and grouted pipe dowels of roughly 1.5 inches in diameter.

Performance parameters being measured include: construction costs and features (including dowel bar position verification using ground penetrating radar), load transfer measured by FWD testing, faulting, cracking, spalling, and traffic loading. In addition to the field testing, laboratory testing is also being performed to determine the material properties, durability, and pullout strengths of the dowels. The testing and observations are scheduled for completion in a five-year period. The test program began in 1998.

3. DESCRIPTION OF THE MINNE-ALF TEST PLATFORM AND CURRENT TEST PROGRAM

3.1 Development of the Minne-ALF

This chapter gives a brief overview of the development of the Minne-ALF test platform and test program. More detailed information can be found in references 2, 3, and 4.

In 1994, the Minnesota Department of Transportation commissioned the University of Minnesota to develop an accelerated test platform for rapidly and accurately evaluating the long-term performance potential of various highway pavement structural designs and features. This project was developed under the direction of Professor Mark Snyder with the help of Mn/DOT, research fellow Rebecca Embacher and graduate research assistants Micheal Beer, Josh Mauritz, and Eric Embacher.

Field testing is an accurate way of assessing long-term performance potential, but there are many problems involved with this technique, including: high expense of construction and testing, long periods of time required to obtain data, and the poor reliability and dependability of sensors in the given environment for long periods of time. An example of field testing that illustrates these concerns, is the Minnesota Road Research Project (Mn/ROAD) (2). The Mn/ROAD test facility opened in 1994 at a cost of 25 million dollars. It contains thousands of sensors that are connected to a centralized data acquisition network. The projected life expectancy of the facility at the time of construction was approximately twenty years (2). Currently, a large portion of the sensors that were originally installed have already failed.

An alternative to field-testing is “small-scale” laboratory testing. The issue of concern involved with this type of testing is the accuracy in predicting long-term performance potential based on a limited amount of data. Typically, this type of testing only tests the material properties and does not address the pavement system as a whole, making it difficult to predict long-term performance potential of the system.

This project was established to directly address the deficiencies of performance testing and evaluation using long-term field and laboratory tests by developing a test stand that could evaluate full-scale test specimens very rapidly. At the onset of the project, extensive research was conducted to identify design concepts and criteria for the development of the test facility. Information concerning twenty-two existing accelerated load facilities was considered to develop design criteria presented in table 3-1 for the Minnesota Accelerated Loading Facility (Minne-ALF)(2).

Table 3-1 Summary of Minne-ALF Design Requirements

Capability / Feature	Necessary	Desirable
Laboratory / Field		
Laboratory pavement testing	x	
Transportable to field for in situ pavement testing		x
Field power supply		x
Easily upgradable for possible future needs	x	
relatively low initial cost	x	
Pavement Types		
Test rigid pavement	x	
Test flexible pavements		x
Test aggregate pavements		x
Evaluate various pavement design methodologies	x	
Evaluate pavement rehabilitation techniques	x	
Evaluate rigid pavement load transfer devices	x	
Traffic Load Simulation		
Apply 125,000+ critical loads per day	x	
Simulate actual traffic velocity (88 km/h (55mph))		x
Max wheel load of at least the legal limit	x	
Evaluate half-axle loading (reduce specimen cost)	x	
Evaluate full-axle loading		x
Evaluate full-scale pavement sections	x	
Simulate traffic wheel wander		x
Simulate various tire pressures		x
Evaluate various vehicle suspension system		x
Pavement Base/Foundation		
Utilize natural pavement foundation material	x	
Utilize artificial pavement material	x	
Test base material of various permeability		x
Examine subgrade pumping mechanism		x
Environmental Effects		
Examine moisture gradients in rigid pavement		x
Examine temperature gradients in rigid pavement		x
Examine freeze/thaw cycle effects		x
Window to observe pumping in subgrade		x
Test various pavement drainage devices		x
Test pavement with flooded base material		x

It was determined that a linear loading type of design would be the most cost-effective and appropriate for the desired testing. Three preliminary linear loading type designs were examined including a load cart attached to a long-stroke hydraulic actuator, multiple vertical actuators aligned in series, and two vertical actuators connected to a rocker beam.

The third design was considered the most feasible of the three designs. It used two vertically oriented actuators, which were hung from the bottoms of two large bents attached to a steel foundation frame. The opposite ends of the actuators were attached to the ends of a nine-foot, W10 x 68 steel beam. At the bottom of the beam, a large radius aluminum arc was attached. This allowed for the rocking motion to be produced by applying alternating forces to the ends of the beam. Figures 3-1 and 3-2 are elevation drawings of the original test platform (2).

After construction was completed, the initial testing began. It soon became apparent that the existing test configuration and control system would not allow the simulation of a relatively constant 9-kip single-wheel load at required testing speeds (3). The problem was linked to action-reaction responses of the actuators. When one actuator applied a load, it caused a reaction in the other. This required the control system to modify the actuator response in order to maintain the desired load. At higher speeds, the control system was not fast enough to make the proper response adjustments, causing the applied load to fluctuate significantly from the desired levels. Consequently, major modifications of the test stand were made. These modifications included changing the rocker beam and actuator configurations, stiffening the frame, modifying the hydraulic supply system, and upgrading the actuator control system (3,4).

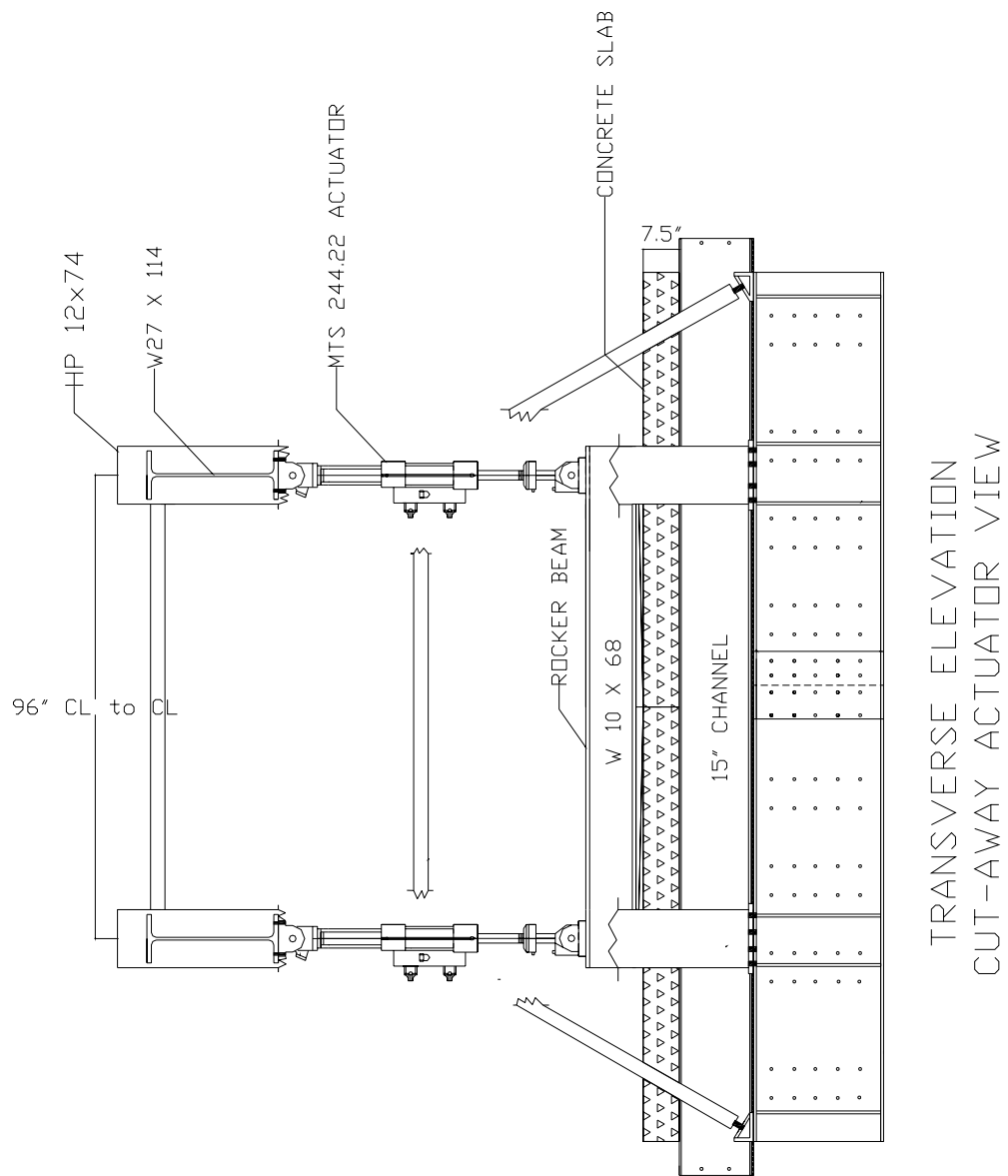


Figure 3-1 Transverse Elevation of Original Minne-ALF Test Stand Design (2)

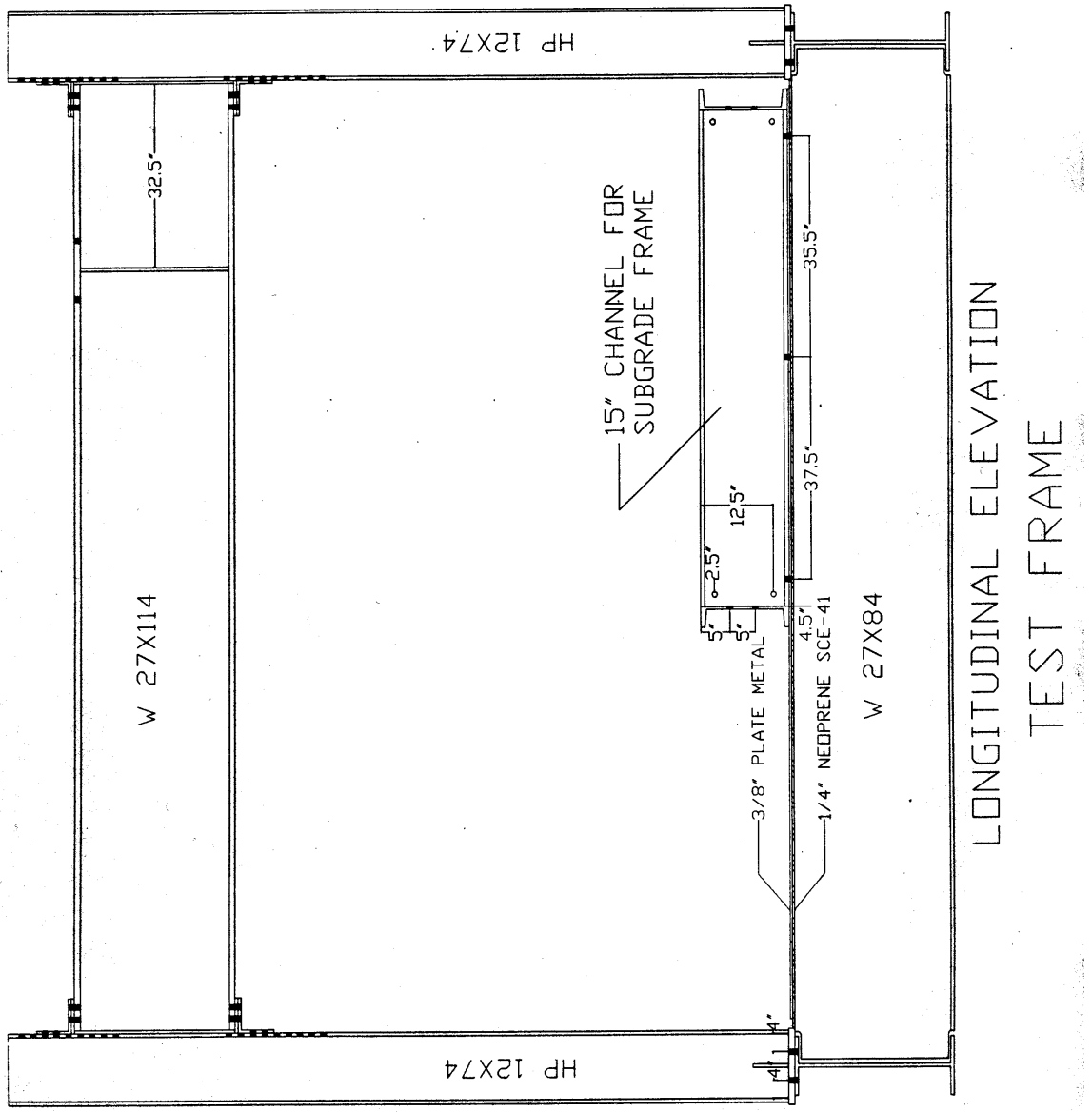


Figure 3-2 Longitudinal Elevation of Original Minne-ALF Test Stand Design (2)

3.2 Current Minne-Alf Test Setup

3.2.1 Capabilities of the Current Minne-ALF Test Setup

The overall objective of the Minne-ALF test platform design was to accurately simulate the loading effect caused by heavy vehicles traveling at highway speeds on a pavement test section. In order to achieve this, major modifications were performed on the original test platform, as previously discussed.

The current test stand is illustrated in Appendix A, and table 3-2 summarizes the capabilities of the current Minne-ALF test setup (3). Each load cycle simulates the passage of one-half of one axle of a heavy vehicle traveling across the test specimen. It consists of a 9-kip load traveling from one end of the test rocker beam to the other (a total load path of 9 feet). The specimen is subjected to loads traveling in one direction only because unidirectional loading is most common in highway pavements and because it is an important aspect of the pumping mechanism that may develop if adequate load transfer is not provided. The 9-kip load represents half of the maximum single axle load (18,000 lbs) allowed in Minnesota and corresponds to the size of the test specimens currently in use (6 feet wide, or one half of a twelve-foot lane). A small load (2 kips) is used on the return portion of the load cycle to ensure constant contact between the rocker beam and the pavement surface, thereby eliminating the possibility of impact loading on subsequent load cycles. The system currently operates using a 1.5-hertz load cycle, which equates to 129,600 load cycles a day at an average loading rate of 21 mph. The actual speed as the load crosses the center of the test specimen is approximately 30 mph. A load frequency of 2 hertz was used during initial tests, which allowed for faster load applications. However, the repeated failure of some of the hydraulic components led to a reduction in load frequency to 1.5 hertz. Higher load speeds and frequencies are possible with upgraded hydraulic components and minor test frame modifications. The size of the test specimen and the magnitude and type of loading can be easily changed to simulate other test conditions.

The current test stand meets all of the initial design requirements and is now being used to evaluate the long-term performance potential of rigid pavement designs and rehabilitation techniques.

Table 3-2 Desired and Existing Minne-ALF Capabilities (2)

Capability / Feature	Necessary	Desirable	Has	Possible w/ expansion	Not possible
Laboratory / Field					
Laboratory pavement testing	x		x		
Transportable to field for in situ pavement testing		x		x	
Field power supply		x		major	
Easily up-gradable for possible future needs	x		x		
relatively low initial cost	x		x		
Pavement Types					
Test rigid pavement	x		x		
Test flexible pavements		x		minor	
Test aggregate pavements		x		minor	
Evaluate various pavement design methodologies	x		x		
Evaluate pavement rehabilitation techniques	x		x		
Evaluate rigid pavement load transfer devices	x		x		
Traffic Load Simulation					
Apply 125,000+ critical loads per day	x		x		
Simulate actual traffic velocity (88 km/h (55mph))		x		minor	
Max wheel load of at least the legal limit	x		x		
Evaluate half-axle loading (reduce specimen cost)	x		x		
Evaluate full-axle loading		x		minor	
Evaluate full-scale pavement sections	x		x		
Simulate traffic wheel wander		x		major	
Simulate various tire pressures		x		major	
Evaluate various vehicle suspension system		x			x
Pavement Base/Foundation					
Utilize natural pavement foundation material	x		x		
Utilize artificial pavement material	x		x		
Test base material of various permeability		x	x		
Examine subgrade pumping mechanism		x	x		
Environmental Effects					
Examine moisture gradients in rigid pavement		x		minor	
Examine temperature gradients in rigid pavement		x		minor	
Examine freeze/thaw cycle effects		x		major	
Window' to observe pumping in subgrade		x		minor	
Test various pavement drainage devices		x		minor	
Test pavement with flooded base material		x	x		

3.2.2 Description of Test Stand and Hydraulic System

The current test stand uses many of the components from the original test platform. A complete set of drawings illustrating the current setup can be found in Appendix A.

The base consists of nine W27 x 84 transverse beams connected to two W27 x 84 longitudinal beams that rest on the laboratory floor. On top of the beams is a $\frac{1}{4}$ -inch layer of neoprene and 3/8-inch steel plate. Fifteen-inch steel channels that lie on top of the steel plate enclose the test specimen foundation. The foundation is made of a 3-inch layer of Mn/DOT class 5 material on top of a 9-inch layer of clay-loam, which rests upon a $\frac{1}{4}$ -inch layer of neoprene. This represents a scaled approximation of the foundation found in test section 6 at Mn/ROAD (4), which features 5 inches of class 4 material.

The loading is applied to the test specimen by two independently controlled hydraulic actuators connected to a rocker beam. The rocker beam consists of a nine-foot. W10 x 68 steel beam with a large radius aluminum arc attached to the bottom. At one end of the beam, a roller bearing system is attached that allows for the proper positioning and movement of the rocker beam. The beam also has two other lateral guidance fixtures at the center and opposite end of the beam. The load is applied by a 22-kip “load-controlled” vertical actuator that is connected to a 26-inch long W10 x 60 steel section mounted perpendicularly to the rocker beam at it’s mid-point. The rocking action is accomplished by a 22-kip “stroke-controlled” horizontal actuator, which is attached perpendicularly to the top of the previously mentioned W10 x 60 section. The opposite ends of the actuators are connected to horizontal crossbeams that allow the frame to be “self stressing”. Diagonal lateral braces stiffen the platform.

The actuators are powered by a hydraulic pump system capable of supplying 150 gpm at an operating pressure of 3,000 psi. A hydraulic service manifold (HSM) connects the Minne-ALF hydraulic system to the laboratory’s main hydraulic lines. The HSM increases the uniformity of the hydraulic flow and allows other hydraulic testing equipment to be unaffected by the Minne-ALF testing (and vice-versa). The actuators are connected to the HSM by 1-inch inside diameter, flexible hydraulic hoses. The flow in and out of the actuators is controlled by two 15 gpm electronic servo-valves, which are controlled by an MTS Teststar system.

3.2.3 Description of Test Control and Data Acquisition Systems

The hydraulic actuators are controlled by the MTS Teststar System. The system consists of a personal computer operating under Windows NT, and a Teststar controller. The system uses MTS Teststar and TestWare computer software. The system works by first sending command signals to the actuators. The command signal is generated from a text file containing 1024 points that describe the desired waveform needed to produce the correct motion and loading of the rocker beam (3). The horizontal or “stroke-controlled” actuator uses a “haversine waveform” and the vertical or “load-controlled” actuator uses a “square waveform” that varies from 9 kips to 2 kips. Figure 3-3 presents a plot of the waveforms used to generate the command signals.

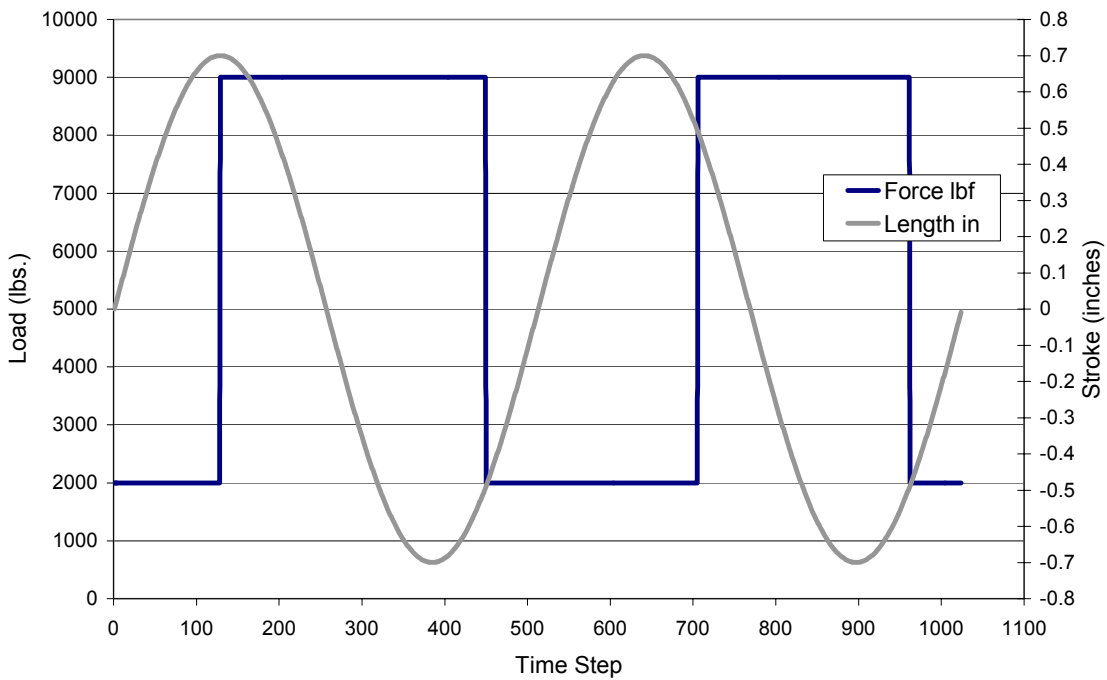


Figure 3-3 Plot of Command Waveforms

After the signals are sent, “feedback” load and displacement signals are sent back to the computer from load cells and linear variable displacement transducers (LVDTs) in the actuators. The software adds a correction factor to the command signal. This reduces the difference, or error, between the feedback and command signals. The process is then iterated. When the difference between the desired load profile and the actual load profile becomes very close, the computer is instructed to save the last iteration. This last iteration is known as the “drive-file”. The “drive-file” is then continuously replayed producing identical load cycles. Prior to testing, a “shakedown” is performed on the system. During this process, a high frequency “white noise” signal is sent through the system and the response is measured. This response is then used to generate the correction factors used in the iteration process.

The software also controls data acquisition. Data is taken from both internal sources (actuator load cells and internal LVDT’s) and external sources. Currently, two external LVDTs (measuring slab displacement) are connected to the Teststar controller, but the system is capable of reading a large number and variety of external sensors. Data can be taken both manually and automatically. The software allows for data collection at user-defined intervals. When the data acquisition system is triggered (either manually or automatically), 800 lines of data are taken at a rate of 400 hertz and saved to a Microsoft Excel spreadsheet. This file can then be downloaded from the computer.

3.3 Verification of Minne-ALF test program

3.3.1 Introduction

After completion of the test stand modifications and test program refinement, demonstration testing was performed. The following sections describe the testing that was performed, along with the results and conclusions. The test procedures described below are consistent with those used in the current test program and are described in detail in chapter 4 of this report. The testing (4) was performed to:

1. Determine the effects of selected design and construction variables on retrofit dowel load transfer system performance,
2. Determine the variability of Minne-alf test results,
3. Demonstrate the general usefulness of the Minne-alf,
4. Identify the need for any additional test modifications.

3.3.2 Description of Testing and Test Specimens

The design parameters considered in the demonstration testing focused on load transfer mechanisms in cracks and joints. The testing was performed on six PCC pavement test specimens retrofitted with 1.5-inch diameter, epoxy-coated, mild steel dowel bars. Load transfer efficiency (LTE) and differential deflection were used as the criteria for comparing the performances of the test specimens. All specimens were tested on the composite foundation previously discussed. The dimensions of the specimens measured 15 feet in length, 6 feet in width, and 7.5 inches in depth. The concrete used to cast the specimens was a typical Minnesota paving mix (4).

Specimen 1 was a precast slab that was transported to the test stand and positioned on the test foundation. A full-depth transverse crack, located at approximately mid length, was made by repeated loading of the 22 kip vertical actuator (without rocking) through a modified load plate. Three 18-inch long dowel bars, spaced at 6 inches from the edge and 12 inches on center, were then retrofitted across the crack. A Mn/DOT 3U18 grout material was used to backfill the dowel slots.

Due to the difficulty in leveling the first specimen, specimens 2 through 6 were cast in place on the test foundation. Plywood with a $\frac{1}{4}$ -inch thickness was used to produce smooth transverse joints at the centers of the slabs for these test specimens. This required that the load transfer be provided exclusively by the retrofitted dowel bars. Specimen 2 was essentially the same as specimen 1 except for the use of the preformed smooth joint that replaced the tight crack.

Specimen 3 was a replicate of specimen 2. The fourth specimen featured the same design as specimens 2 and 3, but used Speed Crete 2028, a proprietary backfill material, as an alternative to the 3U18 backfill material. Specimen 5 was a replicate of specimen 4, but utilized 15-inch long dowels as an alternative to the 18-inch dowels used in fourth specimen. The sixth test specimen was the same as the fifth specimen except stainless steel clad dowels where substituted for the epoxy-coated, mild steel dowels.

The slabs were tested using the Minne-ALF test platform and test program. The test program consisted of casting the slabs, retrofitting the dowel bars, loading the test specimens, collecting the test data and performing a data analysis. Details of the test procedures can be found in Chapter 4. Six days after the slabs were cast, the dowel bars were retrofitted. For the first specimen, retrofit took place one year after casting, due to delays in completing test stand modifications. One day after the dowels were installed, a 9-kip unidirectional moving load was applied to the test specimens at a cycle rate of 2 hertz. Testing continued until LTE dropped below 70 percent and differential deflection increased to over 5 mils. Load, stroke and slab deflection data were taken at 50, 100, 1000, 2000, 5000, 10000, 20000, 50000, 100000, 300000, 600000 load cycles and every 600000 load cycles thereafter (4). Each data collection effort consisted of 2 seconds of data sampled at 400 hertz, which equates to 800 lines of data for four full load cycles. Stroke of the horizontal actuator, load of the vertical actuator, time, and two slab displacement readings were taken for each line of data. The slab displacement readings were measured by external LVDT's positioned close to the joint.

3.3.3 Results

Differential deflection and LTE were computed from the collected data. From each 800 line data series, four values of LTE and differential deflection were computed. The lines used to determine LTE and differential deflection were taken when the 9 kip load was centered approximately 6 inches from either side of the joint or crack on the loading portion of the two included cycles. The six-inch distance corresponds to similar load placement in falling weight deflectometer (FWD) testing in the field. The four values were averaged and plotted on a semi-log chart. Figures B-1 through B-8 in Appendix B (4) present the test results for the six test specimens.

Using this information Embacher and Snyder were able to make the following recommendations and conclusions (4):

- It appears that the Minne-Alf is a useful tool for evaluating the relative performance of rigid pavement designs and design features. It provided comparable test results for the two replicate specimens that were tested and it indicated significantly improved performance when load transfer was provided by both retrofit dowels and very good grain interlock.
- The LTE and differential deflection histories for the slab containing speed crete 2028 concrete backfill is greatly improved over those measured for test slabs containing 3u18 concrete backfill with similar joints and dowel bars. This could be due in part to the higher initial strength of speed crete 2028 concrete backfill.
- At this time the effect of dowel bar length could not be properly determined due to poor consolidation. Additional tests should be performed to examine the effects of dowel length and dowel materials on the performance potential of retrofit (and original construction) load transfer systems.
- It appears that the load carrying capabilities of the slab were unaffected by the use of stainless steel-clad dowels in lieu of epoxy-coated structural steel dowels.
- Minor modifications and standard maintenance practices are recommended to allow the Minne-ALF to run more effectively.
- 3u18 concrete backfill sack mix should no longer be used due to large inconsistencies between sacks. The backfill material should be obtained by manually proportioning the 3u18 concrete mixes.

4. DESCRIPTION OF RESEARCH PROGRAM AND TEST PROCEDURE

4.1 Introduction

The testing performed in this research project utilized the previously established Minne-ALF test program and test procedures. A complete description of test variables, measures of performance, test specimens, procedures, and data acquisition is provided in this chapter. Background on the Minne-ALF test program, including descriptions of the test platform and load simulation, can be found in the previous chapter.

4.2 Test Variables

To address the problems of the high cost of retrofit load transfer and dowel bar corrosion, two different design variables were tested. These variables included dowel bar material and design configuration. To test these variables, four different retrofit dowel bar designs were selected. The designs that were tested were chosen due to their cost effectiveness and likelihood of use in the field. The first three designs featured the same design configuration, but vary in dowel bar material. Noncorroding material was used in two of the designs to address the problem of dowel bar corrosion. The fourth design is similar to the first design in material but varies in geometric configuration. This design addresses high retrofit cost and the problems associated with load transfer restoration of thin concrete pavements.

4.3 Measures of Comparison

4.3.1 *Introduction*

The criteria used for comparing the performance of the retrofit designs were based on three performance measures: LTE, differential deflection and observed behavior (such as cracking).

4.3.2 LTE

One measure of load transfer is load transfer efficiency or LTE, which is “the ability of a joint or crack to transfer load from one side of the joint or crack to the other”(1). It is computed from measured displacements of the slabs in the vicinity of the joint when a load is applied to one of the slabs. The values for LTE reported in this study were computed using the deflection LTE equation 2-1. The use of this equation for determining LTE was based on its wide acceptance.

4.3.3 Differential Deflection

Differential deflection is the relative displacement between the loaded and unloaded sides of the joint or crack. It is computed by taking the difference of the displacements, as suggested by Equation 2-4. Differential deflection is frequently used to provide additional information about the performance of the joint or crack.

4.3.4 Observed Behavior

Observed behavior includes any physical observations made during testing or examination of the specimen during or following testing. During testing, the slab and slots are checked for any visible signs of deterioration. After testing, a core was taken from the slab through the dowel located closest to the slab edge (i.e., the critically loaded dowel) for visual inspection. In

addition, the remaining dowel bars were carefully removed and inspected. Any signs of deterioration were noted and recorded.

4.4 Description of Test Specimens

4.4.1 Test Foundation

The test foundation was a composite foundation made of both natural and artificial materials. The top layer consisted of 3 inches of Mn/DOT Class 5 material. The second layer was a 9-inch layer of clay-loam that was placed above a $\frac{1}{4}$ -inch layer of neoprene. The entire foundation was enclosed by 15-inch deep steel channels and rested on the Minne-ALF test stand, as described in chapter 3. The natural foundation layers were compacted to near maximum density at a moisture content near optimum(3).

4.4.2 Test Slabs

The PCC test slabs were cast in position on the test foundation. They measured 15 feet in length, 6 feet in width and 7.5 inches thick. At the center of the slab, a $\frac{1}{4}$ -inch thick, 7.375-inch tall piece of plywood was placed to form a smooth, full-depth joint transversely across the slab. The intent of this joint was to provide a smooth joint face so that any load transfer capacity was provided solely by the retrofitted dowel bars. The slabs were cast on top of the composite test foundation. A 2 mil thick layer of plastic was placed between the foundation and the concrete to protect the test foundation during removal of the tested slab. The concrete used to cast the slabs was a Mn/DOT 3A41 concrete mix. This is a typical mix used in PCC pavement construction in Minnesota, and was purchased from a local ready mix supplier.

6-inch diameter by 12-inch long test cylinders were cast, in accordance with ASTM C192, at the same time as the test slabs. These cylinders were used for compressive strength and static modulus of elasticity testing which was performed after 1 day, 3 days, 7 days, and 28 days of curing and was performed in accordance with ASTM C39 and ASTM C469, respectively. Tables 4-1 and 4-2 summarize the PCC strength test results.

TABLE 4-1 Summary of Test Slab Compressive Strengths

Days of Curing	Compressive Strengths (psi)																	
	Slab 1					Slab 2					Slab 3					Slab 4		
	Specimen Number			Average	Specimen Number			Average	Specimen Number			Average	Specimen Number			Average		
	1	2	3		1	2	3		1	2	3		1	2	3			
1	1146	1265	1254	1222	2087	2059	1866	2004	1897	1915	1869	1894	1568	1433	1507	1503		
3	2328	2370	2276	2325	2789	3125	2886	2933	2332	2433	2061	2275	3267	3229	2551	3015		
7	3763	3842	3830	3812	3706	3977	3836	3840	3872	3668	3769	3668	4453	4281	3972	4235		
28	5064	4941	5353	5120	4641	4781	4713	4712	3922	3940	3826	3896	5586	5683	5570	5613		

TABLE 4-2 Summary Of Test Slab Static Moduli Of Elasticity

Days of Curing	Static Modulus of Elastisity (ksi)															
	Slab 1				Slab 2				Slab 3				Slab 4			
	Specimen Number			Average	Specimen Number		Average	Specimen Number			Average	Specimen Number		Average		
	1	2	3		1	2		1	2	3		1	2		1	2
1	2380	1920	1790	2030	2960	2610	2785	2460	2590	2530	2527	2490	2470	2760	2573	
3	3150	2470	2840	2820	3140	3110	3125	2900	3000	2790	2897	3410	3320	3700	3477	
7	3280	3210	2970	3153	3850	3500	3675	3660	3600	3270	3510	3540	4040	3980	3853	
28	4030	3980	3910	3973	3840	3710	3775	3740	3740	3480	3653	4520	4670	4790	4660	

4.4.3 Dowel Bar Retrofit Designs

Four different dowel bar retrofit designs were tested. The first design is representative of a typical dowel bar retrofit design used in the state of Minnesota and was used as the standard for comparison with the other three designs. It consisted of three, 1.5-inch diameter, 15-inch long, epoxy-coated, mild steel dowel bars. The first dowel bar was placed 6 inches from the longitudinal edge of the slab. The second and third dowels were spaced transversely at 12 inches on center, from the first dowel. The dowel bars were positioned vertically at the mid-depth of the concrete slab and centered over the smooth, formed joint. The second design was similar to the first design but, utilized 1.5-inch diameter, 15-inch long, fiber-reinforced polymer (FRP) dowel bars. The third design was again similar to the first design, but 1.66-inch diameter, 18-inch long, stainless steel, grouted pipes with a 1/8-inch wall thickness were used for the dowel bars. The fourth design was the same as the first design except that the bars were placed in more shallow slots and were located vertically 1 inch higher in the slab (corresponding to two inches of clear cover instead of three).

The material used for backfilling the slots was Speed Crete 2028, which comes prepackaged in 50-pound bags and is mixed with a CA8 gradation pea stone. The mixing process was performed in accordance with the manufacturer's specifications. This backfill material has a high early strength, and is capable achieving 5,000 psi in 3 hours (8). Four-inch diameter by 8-inch long test cylinders were cast along with the backfilling of the slots, in accordance with ASTM C192. The cylinders were then tested for compressive strength after one day of moist curing. Both the preparation and the testing of the cylinders were completed in accordance with ASTM specifications. Table 4-3 summarizes the compressive strengths of the backfill material.

Table 4-3 Summary of Compressive Strength of Backfill Material

Compressive Strengths of Backfill Material (psi)				
Specimen Number	Slab 1	Slab 2	Slab 3	Slab 4
1	5124 (a)	5278 (b)	3031 (c)	4855 (d)
2	3984 (a)	4690	5445	4253
3	5365	5553	4400	4932
4	5573	6260	5433	5053
5	4768	5941	5195	4956
6	5448	5655	5367	5030
7			5332	4840
8			5193	4792
9			5867	4883
Average	5011	5620	5029	4844

(a) Tested after 20 hours of moist curing

(b) Tested after 19 hours of moist curing

(c) Tested after 16 hours of moist curing

(d) Tested after 14 hours of moist curing

4.5 Description of Data Acquisition

The MTS Teststar controller acquired the data, which were obtained from both internal sources (actuator load cells and LVDTs) and external sources (slab LVDTs). Two external LVDTs were used to measure slab displacements, as shown in figure 4-1.



Figure 4-1 Photograph of LVDTs

The LVDTs used were Lucas model #GCA-121-125, which have an operating range of 0.25 inches and a measuring accuracy of 0.00004 inches. The LVDTs were connected to the MTS Teststar controller via cables and a conditioner box. Data series were automatically collected at 50, 100, 1000, 2000, 5000, 10000, 20000, 50000, 100000, 300000, 600000 load cycles and every 600000 load cycles thereafter. Additional series were obtained manually, including “zero

readings” that were taken approximately every other day. When the data acquisition system was triggered (either manually or automatically), 800 lines of data were taken at a rate of 400 hertz, corresponding to 3 complete load cycles in a 2-second time period. Each line of data provided information concerning the horizontal actuator stroke position, vertical actuator load, time, and the two external LVDT readings. This information was then saved to a Microsoft Excel spreadsheet and was downloaded from the computer.

4.6 Test Procedures

4.6.1 Preparation of Test Specimen

The initial step of the test procedure was preparation of the test specimen. First the test foundation was leveled; any surface irregularities that may have occurred during the removal of the previous slab were repaired. Next, a 2-mil thick layer of plastic was placed over the foundation. The slab forms were then placed in position. The forms were reusable and consisted of 8-inch deep steel channels that were bolted together in the corners. Two $\frac{1}{4}$ -inch diameter steel rods that span transversely through the forms were placed at approximately 3 feet, 9 inches from each end. Clamps were then placed on the rods to secure the forms and prevent the forms from spreading during the casting process. The $\frac{1}{4}$ -inch thick plywood transverse joint was then placed at the midpoint of the forms. The position and alignment of the plywood was secured by five 10-inch long pieces of number 4 reinforcing bar. The reinforcing bars were placed against the joint and hammered vertically into the test foundation. Once the forms had been properly placed, they were wiped down with a form release agent. In addition to preparing the slab forms, seventeen, 6-inch diameter by 12-inch long test cylinder molds were also prepared for casting companion test specimens.

The concrete was then transported from a ready mix plant to the University. Air content and concrete slump were measured upon arrival of the truck. The mix was then tempered to achieve a slump of approximately 4 inches or a water cement ratio of .48. The concrete was then loaded into a concrete bucket dump and transported into position using an overhead crane. The concrete was placed and was consolidated using a spud vibrator. The slab was then struck to the correct thickness and bullfloated. Subsequent hand floating and troweling were performed to produce a smooth surface for the rocker beam to ride on. Two thin-gauge steel plates, measuring approximately 1 inch by 1 inch were set into the concrete at the edge of the slab near the joint to provide hard and smooth contact surfaces for the LVDT measuring tips. Table 4-4 displays the initial LVDT positions relative to the joint and slab edge.

TABLE 4-4 Initial LVDT Positions

Reference Point	Initial LVDT Positions (inches)							
	Slab 1		Slab 2		Slab 3		Slab 4	
	LVDT A	LVDT B	LVDT A	LVDT B	LVDT A	LVDT B	LVDT A	LVDT B
Distance from Edge of Slab	0.50	0.50	0.38	0.50	0.25	0.38	0.25	0.38
Distance from Joint	1.00	5.00	1.25	4.88	2.00	6.00	1.50	5.25

As soon as the surface of the slab was hard enough to touch, the slab was covered with wet burlap and tarps. Moist curing was carried out for the entire seven-day period prior to testing.

The 6-inch diameter by 12-inch long test cylinders were cast concurrently with the test slab and were cured in accordance with ASTM C192.

Once the concrete had hardened sufficiently, typically 3-4 days, the slots were cut into the slab across the joint. The center of the first slot was positioned six inches from the edge of the slab; the other two slots were spaced transversely at 12 inches on center from the first slot. The size of slots used in the first three test specimens measured 2.75 inches in width, 30 inches in length (15 inches on both sides of the joint), and 5 inches in depth. The slots used in the fourth test specimen were similar to the previously described slots but were cut to a depth of 4 inches. The ends of the slots were rounded vertically, matching the radius of the saw blade.. A slot was made by first making two parallel, 30 inch long, longitudinal cuts spaced 2.75 inches apart to a depth of 5 inches, perpendicular to the surface of the slab. These cuts form the longitudinal edges of the slot. The cuts were made using a hand held diamond blade concrete saw. After the cuts were made, the material between the two cuts was removed using a 15-pound pneumatic hammer with a 1-inch wide chisel attachment. Figure 4-2 shows the slots being prepared.



Figure 4-2 Photograph of Slot Preparation

The slots were then cleaned with a steel brush and compressed air. Special attention was given during this process to ensure complete removal of debris and saw slurry. Following the slot preparation, $\frac{1}{4}$ -inch thick pieces of plywood were custom-cut to fit in each slot. This was performed to reestablish the joint through the depth of the slot. A hole corresponding to the diameter of the dowel bar was then drilled into each piece of plywood at a height that allowed for the correct vertical positioning of the dowel. The dowel bars were then fitted with the plywood, end caps, and chairs. Figures 4-3 shows the prepared slots and dowels.



FIGURE 4-3 PHOTOGRAPH OF DOWEL BARS AND SLOTS PRIOR TO RETROFITTING

Prior to retrofitting, the dowel bars were coated with form release agent. After six days of moist curing of this slab, the dowel bars were retrofitted. The process followed during retrofitting was in accordance with Mn/DOT rehabilitation specifications. First, a bonding agent consisting of equal parts of sand and cement was mixed with enough water to give it a “peanut butter-like” consistency. This bonding agent was then applied to the slots. Two 50-pound sacks of Speed Crete 2028 were mixed with 100 pounds of CA8 pea gravel and 11.1 pounds of water. The material was mixed in a standard concrete mixer. The mixing was performed in accordance with the manufacturer’s specifications. The slots were then backfilled with the material in three lifts. Care was taken to ensure that proper positioning of the dowel bars was maintained. Each lift was vibrated using a spud vibrator. Subsequent to filling the slot and consolidating the backfill material, finishing was performed using a wood float and hand trowel. The 4-inch diameter by 8-inch long test cylinders were cast concurrently with the backfilling of the slots. As soon as the surfaces of the slots were hard enough to touch, they were covered with wet burlap and tarps. Moist curing was performed for 1 day. After the slots had cured for approximately 15 hours, and prior to applying any load to the slab, a few selected test cylinders were tested for compressive strength. If the cylinders had a compressive strength of 3,000 psi or higher, assembly of the test system began. For all specimens tested, a 3,000 psi compressive strength was achieved. Mn/DOT specifications require that the backfill material have a compressive strength greater than or equal to 3000 psi within 24 hours of placement (7). Since testing begins 24 hours after retrofitting the dowel bars, preliminary strength tests were performed to allow for assembly of the test system.

4.6.2 Assembly of Test System

Assembly of the test system was required before testing could begin. First, the rocker beam was installed on top of the burlap and tarps. The beam was centered directly over the outermost dowel (i.e., over the critical dowel). All of the lateral guidance fixtures were then installed. The hydraulic actuators were then lifted into position and securely fastened. Additional lateral bracing was then mounted. Careful alignment of the all the components was required to produce the proper rocking motion and loading of the test slab. The actuator cables were then connected. The cables and hydraulic hoses were fastened to the frame and padded to prevent chafing. The hydraulic power was turned on and the beam was raised to remove the burlap and tarps. An 11-

inch wide urethane-poron pad was then placed under the rocker beam and the beam was lowered. The LVDT stands were positioned. The roller bearings were greased and all the bolts were checked for tightness. The test system was then ready for calibration and testing. Figure 4-4 shows the test platform and test specimen prior to testing.

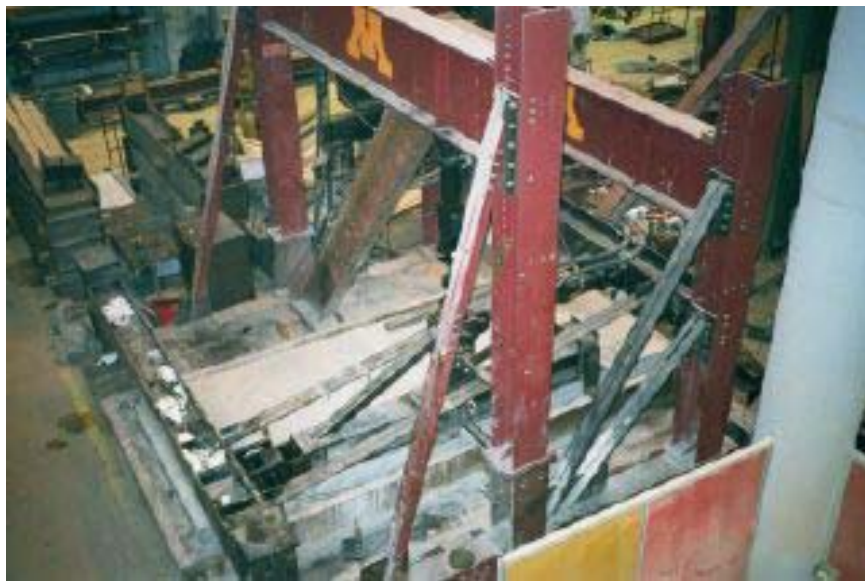


Figure 4-4 Photograph of Minne-ALF Prior to Test

4.6.3 Calibration of Test System and Pretest Procedures

Prior to testing, the system required calibration. First, the LVDTs were calibrated using the manufacturer's specifications. The Teststar controller was then calibrated. This process involved adjusting the Teststar sensor range to produce an output of ± 10 volts and computing the Teststar voltage offset for each LVDT (4). This calibration process ensured that the readings measured by the LVDT corresponded to Teststar readings, which were used for analysis. Once this calibration was complete, the LVDTs were positioned in their stands. They were set such that their readings were close to the mechanical zeroes.

A drive file used by the system to create the loading was then created. The rocker beam was first leveled using the hydraulic controls and a 4-foot carpenter's level. Once the beam was level, the horizontal actuator's stroke was zeroed. This was performed to enable the proper rocking motion of the beam, the command waveforms are based on the fact that when the beam is directly over the joint the stroke is zero. Using the Testware software an inverse transfer function (ITF) file was then created; this is known as a "shake down" procedure. During this process, a 15-hertz signal with a range of frequency components, known as "white noise", was sent through the system and the response was measured. This response was then used to form the correction factors used during the iteration process to establish a load profile. The iteration process was then performed and a drive file was created. This drive file was then continuously replayed to produce the desired loading of the test specimen. A more detailed account of this procedure is described in chapter 3. Before testing was begun, "zero readings" were obtained from the LVDTs.

5. RESULTS and ANALYSIS

5.1 Data Analysis

An analysis was performed on the test data. First, the MTS TestStar data acquisition software converted the data from analog to digital voltages. The software then corrected the data for the initial voltage offsets and converted it to the necessary units (i.e., measurements of force or length). The data were then saved in Microsoft Excel spreadsheet format and downloaded from the Minne-ALF computer for analysis.

For each of the 800-line data sets, the slab displacement data were adjusted by the appropriate LVDT zero displacement values to produce actual displacement measurements. In addition, total cumulative load cycles, LTE and differential deflection were computed for each data set. The equations used to compute LTE and differential deflection are equations 2-1 and 2-4, respectively, and a description of these equations can be found in chapters 2 and 4.

Data sets were taken at approximately 50, 100, 1000, 2000, 5000, 10000, 20000, 50000, 100000, 300000, 600000 load cycles and every 600000 load cycles thereafter. Four graphs were plotted for each data set to show approach LTE, leave LTE, differential deflection, and the load profile. These graphs were used as quality checks of the data, and were used to aid in troubleshooting any problems with the data or testing system. The approach side is a reference to the “upstream side” of the joint with respect to the unidirectional load, in the current Minne-ALF test setup it is the west side of the joint. Similarly, the leave side is a reference to the “downstream side” of the joint with respect to the unidirectional load, which is the east side of the join in the current Minne-ALF test setup it. From each data set, three values of load, LTE, and differential deflection were computed and averaged. These averaged values were then plotted on two semi-log graphs: LTE versus number of applied load cycles, and differential deflection versus number of applied load cycles. The lines used to determine LTE and differential deflection were taken when the 9-kip load was approximately 6 inches from the joint on the approach side. This corresponds to standard testing practice in the field when using a FWD, which employs a 300-mm (12-inch) diameter load plate placed next the joint.

5.2 Results

5.2.1 Influence of Changing Dowel Bar Material

Relative long-term performance potential for designs that used different dowel bar materials was based on a comparison of LTE and differential deflection, along with a post-test examination of the dowel bars and backfill material. Three different dowel bar materials were tested: 1.5-inch diameter, 15-inch long, epoxy-coated, mild steel dowels (slab 1); 1.5-inch diameter, 15-inch long, fiber reinforced polymer dowels (slab 2); and 1.66-inch diameter, 1/8- inch thick walled, 18-inch long, grouted stainless steel pipe dowels (slab 3). The results of the three tests are summarized in Table 5-1 and are shown in Figures 5-1 and 5-2. Slab 1, containing the epoxy-coated steel dowels, was used as a control for the other test specimens. The data for the first 300,000 load cycles of slab 1 was lost due to a problem with the data acquisition system. Testing on this slab continued for 10.5 million load cycles, past the standard cutoff of 6.7 million load cycles. This was done because it was the control for this study and would be used as a basis of comparison for future Minne-ALF load transfer studies. Slab 3 and Slab 4 were also tested past the standard cutoff point to 13.4 million load cycles. This was done at the funding agency’s request.

Table 5-1 Summary of Test Results

Applied Load Cycles (millions)	Slab 1 1.5 inch diameter, 15 inch long, epoxy-coated dowels placed at mid depth		Slab 2 1.5 inch diameter, 15 inch long, FRP dowels		Slab 3 1.66 inch diameter, 1/8 inch thick walled, 18 inch long, grouted stainless steel dowels		Slab 4 1.5 inch diameter, 15 inch long, epoxy-coated dowels placed at 2 inches below surface	
	LTE (%)	Differential Deflection (mils)	LTE (%)	Differential Deflection (mils)	LTE (%)	Differential Deflection (mils)	LTE (%)	Differential Deflection (mils)
0.00005					95	1.2	94	1.3
0.0001					95	1.2	93	1.6
0.001			92	1.9	95	1.3	94	1.6
0.002			92	1.8	95	1.2	93	1.7
0.005			91	2.1	95	1.4	94	1.6
0.01			91	2.2	96	1.4	95	1.5
0.02			91	2.2	96	1.4	94	1.7
0.05			93	2.4	95	1.4	95	1.5
0.1			93	2.7	96	1.3	95	1.5
0.3			86	3.1	94	2.1	94	1.7
0.4	94	1.6						
0.5							93	1.9
0.6			86	3.9	96	1.4	95	1.7
0.7	95	1.6						
0.8							94	1.7
1.2	95	1.6	82	4.8	96	1.6		
1.5							94	2.6
1.8	96	1.5	84	4.2	95	1.8		
2.0							94	2.0
2.4	96	1.5	84	4.4	95	1.8	94	1.8
2.9	96	1.4						
3.0			83	4.7	96	2.0	93	2.2
3.3	94	1.7						
3.6	95	1.6	83	4.9	95	2.1	94	2.1
4.2	95	1.5	85	4.9	94	2.8	93	2.6
4.8			86	4.9	93	2.9	92	2.4
5.4			82	4.6	94	3.0		
6.0					94	2.7		
6.2			82	4.8				
6.4			84	4.9			92	2.4
6.6	95	1.8	83	4.8	95	2.5		
6.7			82	4.9				
6.8	93	2.2						
7.0	93	2.2						
7.2					94	3.1	92	2.5
7.6	93	2.2						
7.8					94	2.9		
8.1	93	2.2						
8.4					92	3.7	93	2.3
8.7	92	2.4						
9.0							92	2.5
9.6	93	2.3					91	2.6
10.2							91	2.4
10.3					91	3.9		
10.5	93	2.2						
10.8							92	2.7
11.0					93	2.9		
11.4					93	3.1	93	2.5
12.0					92	3.2	91	2.6
12.7					89	4.9	92	2.6
13.0					85	5.9		
13.2					87	5.2		
13.5					86	5.5		

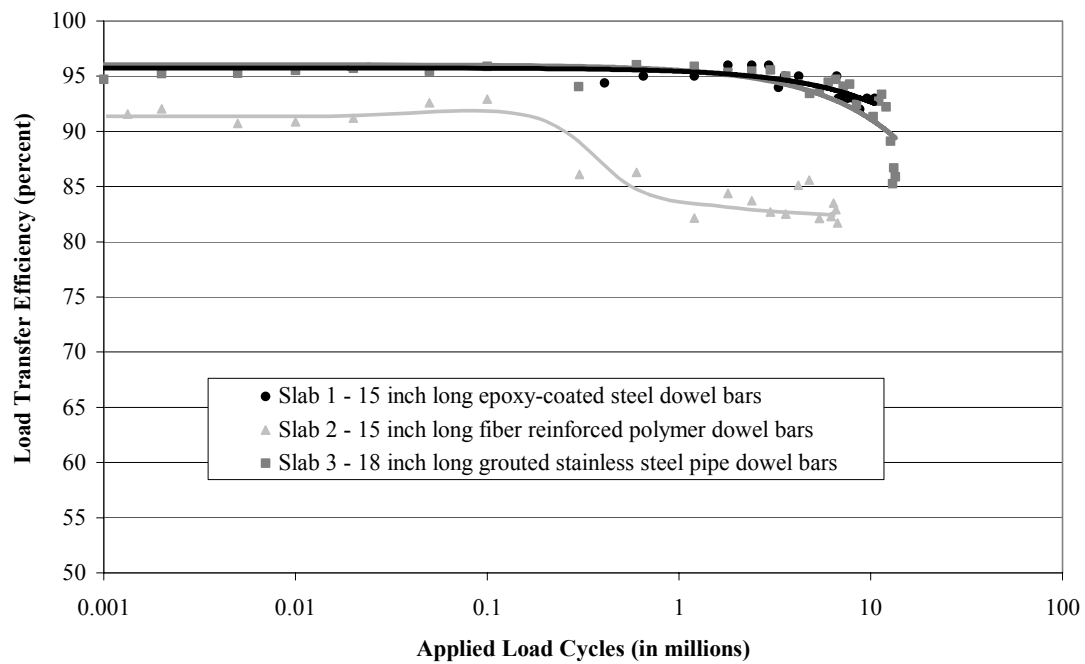


Figure 5-1 Influence of Changing Dowel Bar Material on Load Transfer Efficiency

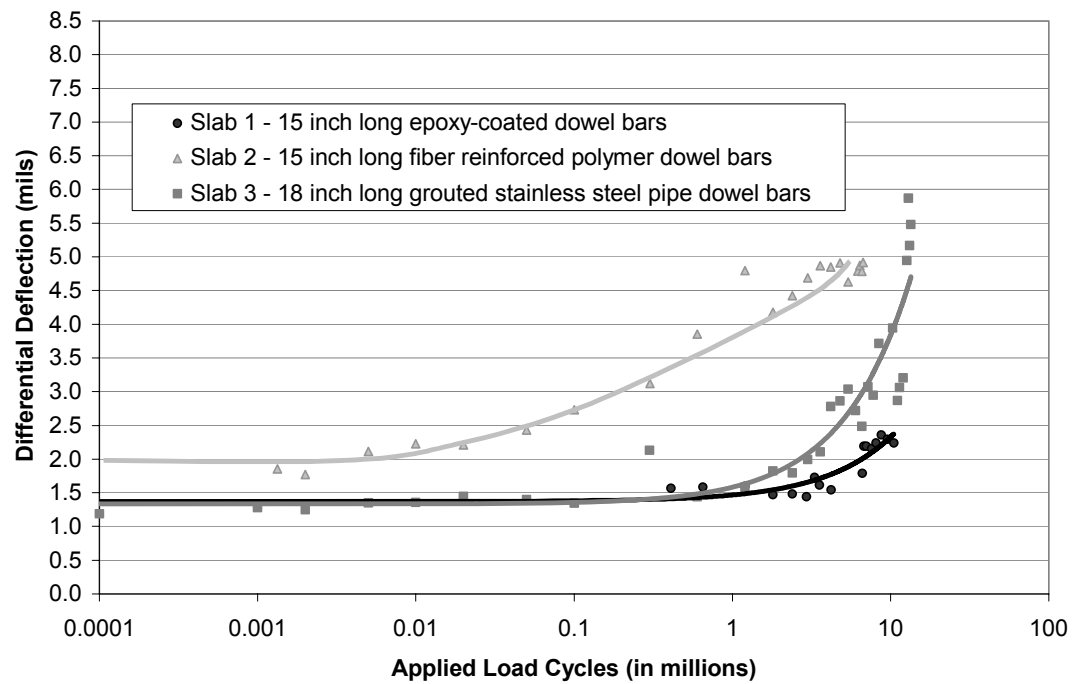


Figure 5-2 Influence of Changing Dowel Bar Material on Differential Deflection

Based on the three performance measures (LTE, differential deflection, and observed behavior), slab 1, containing the epoxy-coated steel dowels, outperformed slab 2, containing the FRP dowels. The LTE for slab 2 began at 92 percent and dropped off significantly to the 84 – 86 percent range after 300,000 load cycles. It then continued to drop off at a much slower rate until reaching 82 percent at the termination of testing after 6.7 million load cycles. Conversely, slab 1 started with an LTE of roughly 95 percent and maintained this level through 6.7 million load cycles, dropping only 2 percent during 10 million cycles of testing. Comparing the differential deflection results, slab 2 started at a slightly higher differential deflection, but it increased to approximately 3 times the amount measured for slab 1 after 2.4 million load cycles. The differential deflection for slab 2 at 6.7 million load cycles was 4.9 mils compared to 1.8 mils for slab 1.

Following testing the dowel bars for both slabs were carefully removed and a visual inspection was performed. A core was also taken through the joint at the critical dowel bar (the one closest to the longitudinal slab edge). After close inspection, it was determined that there was no significant or visible deterioration of the load transfer system in either of the two slabs. Both specimens exhibited fairly good consolidation of the backfill material with no visible signs of deterioration. A small amount of unconsolidated backfill material was present underneath the critical dowel on the approach side near the joint in slab 1. The majority of the backfill underneath this dowel had good consolidation, and the unconsolidated region extended only a short distance on one side of the joint.

Inspection of the dowel bars revealed no major signs of deterioration. A small amount scoring was present at the top of the critical FRP dowel, perpendicular to the major axis of the dowel, where it crossed the joint. No scoring was present on the other FRP dowel bars.

The lower performance of slab 2, as compared to slab 1, is attributed to the lower stiffness in the FRP dowel bars. This concept is supported by the theoretical model used to determine differential deflection of a doweled PCC joint developed by Timoshenko and Friberg. Timoshenko determined that a load P_t applied to a dowel bar in concrete will result in the deflection shown in figure 5-3, and can be computed using equation 5-1 (16):

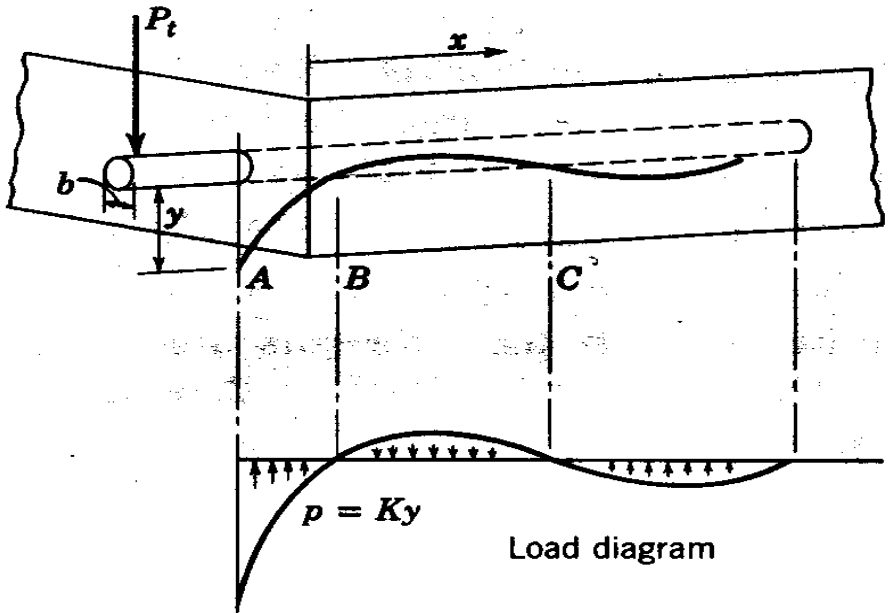


Figure 5-3 Pressure Exerted on Loaded Dowel (16)

$$y = \frac{e^{-\beta x}}{2\beta^2 EI} [P_t \cos \beta x - \beta M_o (\cos \beta x - \sin \beta x)] \quad (5-1)$$

where:

E = natural logarithm base;

X = distance along dowel from face of concrete;

M_o = bending moment on dowel at the face of the concrete;

P_t = transferred load;

E = modulus of elasticity of the dowel;

I = moment of inertia of the dowel; and

β = the relative stiffness of a bar embedded in concrete.

The relative stiffness factor β is computed using equation 5-2 (16):

$$\beta = \sqrt[4]{\frac{Kb}{4EI}} \quad (5-2)$$

where:

K = modulus of dowel support;

B = diameter of the dowel;

E = modulus of elasticity of the dowel; and

I = moment of inertia of the dowel.

Friberg expanded on this work by developing an equation to determine the bending moment in the dowel bar, equation 5-3 (16):

$$M = -\frac{e^{-\beta x}}{\beta} [P_t \sin \beta x - \beta M_o (\cos \beta x + \sin \beta x)] \quad (5-3).$$

Combining Friberg's bending moment equation and Timoshenko's deflection equation at the location of joint, equation 5-1 simplifies to (16):

$$y_o = \frac{P_t}{4\beta^3 EI} (2 + \beta z) \quad (5-4)$$

where:

- Y_o = the deflection of the dowel at the joint (theoretical differential deflection);
- Z = the joint width opening;
- P_t = transferred load;
- E = modulus of elasticity of the dowel;
- I = moment of inertia of the dowel; and
- β = the relative stiffness of a bar embedded in concrete.

For comparing the theoretical differential deflection of the three different dowel bar materials tested, equation 5-4 was used by varying only the physical properties of the dowel bar types. The physical properties of the dowel bars are listed in Table 5-2.

Table 5-2 Physical Properties of Dowel Bars

	Epoxy-Coated Steel 1.5" diameter	Fiber Reinforced Plastic 1.5" diameter	Grouted Stainless Steel 1.66" diameter 1/8" thick walled
Modulus of Elasticity (ksi)	29,000	5,600	28,000 (a) / 4,030 (b)
Moment of Inertia (in⁴)	0.2485	0.2485	.1787 (a) / .1940 (b)

(a) Stainless steel

(b) Grout

Using this model, the theoretical differential deflection of the FRP doweled test specimen would be approximately 1.5 times that of the steel doweled specimen.

The performance measured in slab 3 was a relatively close match to the measured performance of slab 1. The testing resulted in very similar LTE levels, when equivalent testing durations are compared. This is shown in figure 5-4, which graphically compares the two LTE levels for equal test durations.

Examining the test results for slab 3 for the entire test duration reveals a rapid drop in LTE after roughly 10 million load cycles. This trend is illustrated in figure 5-1. Based on the test results, it is not possible to determine if this behavior is unique, or similar in nature to slab 1 because the testing of slab 1 was terminated after 10.5 million load cycles.

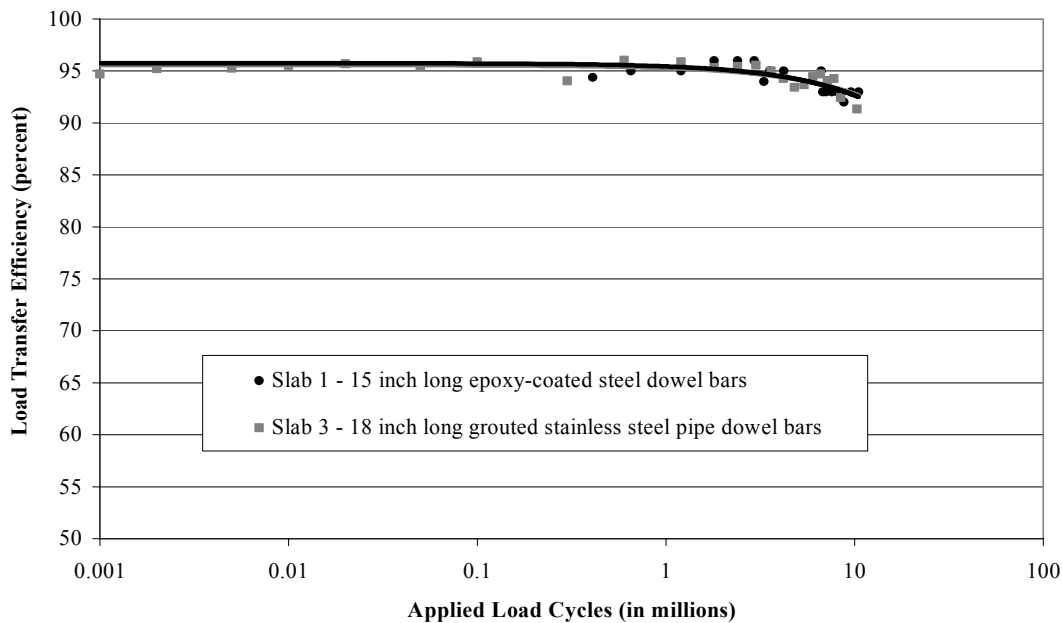


Figure 5-4 LTE Histories for Slabs 1 and 3 for Equal Testing Periods

The difference in measured performance between slabs 3 and 1 is more clearly illustrated in figure 5-2. This plot shows the differential deflection histories for the three dowel bar materials. Comparing slabs 1 and 3, the differential deflection is approximately the same for the first 2 million load cycles; thereafter the differential deflection in slab 3 increases at a greater rate. At 10.2 million load cycles, slab 3 had roughly 4 mils of differential deflection, compared to slab 1, which exhibited approximately 2.2 mils of differential deflection after 10.3 million load cycles. The reason for this difference and sudden drop off in LTE after 10 million load cycles could not be attributed to anything other than inherent variability in test results or actual differences in the performance potential of the two types of bars, with the hollow stainless steel tubes apparently being more prone to early performance deterioration. The stiffness of the grouted stainless steel pipe dowels was approximately 10 percent lower than that of the steel dowels, but the diameter of the grouted stainless steel dowels was slightly larger, thereby canceling out the effect of the lower stiffness. This concept is again supported by theoretical model used to determine differential deflection developed by Timoshenko and Friberg, which yields the same differential deflection for the two test specimens.

A close examination of the test specimens was performed following testing. The dowel bars were carefully removed; both the backfill and the dowels were then inspected. The backfill material was consolidated fairly well and there were no signs of deterioration or “socketing” that could explain the observed behavior. The dowel bars appeared to be in good shape with no visible defects. The dowels were then sent to Mn/DOT, where the grout-filled stainless steel tubes were cut longitudinally to allow inspection of the interior grout. The results of this inspection revealed that little deterioration had occurred in the grout. One hairline crack, perpendicular to the major axis of the dowel was discovered in the grout of the critical dowel.

5.2.2 Influence of Changing Dowel Bar Configuration

The relative long-term performance potential of retrofit dowel bar designs that used different dowel bar configurations was based on a comparison of LTE, differential deflection, and a post-test examination of the dowel bars and backfill material. Two different dowel bar configurations were tested. The first configuration, used in slab 1, used three 15-inch long, 1.5-inch diameter, epoxy-coated, mild steel dowel bars positioned at the mid-depth of the slab, which corresponds to having 3 inches of backfill cover. The second configuration, tested in slab 4, was a replicate of the first configuration except that the dowels were positioned 1 inch higher in the slab, thereby allowing the use of more shallow saw cuts and providing 2 inches of backfill cover. The results of the two tests are summarized in table 5-1 and are shown in figures 5-5 and 5-6.

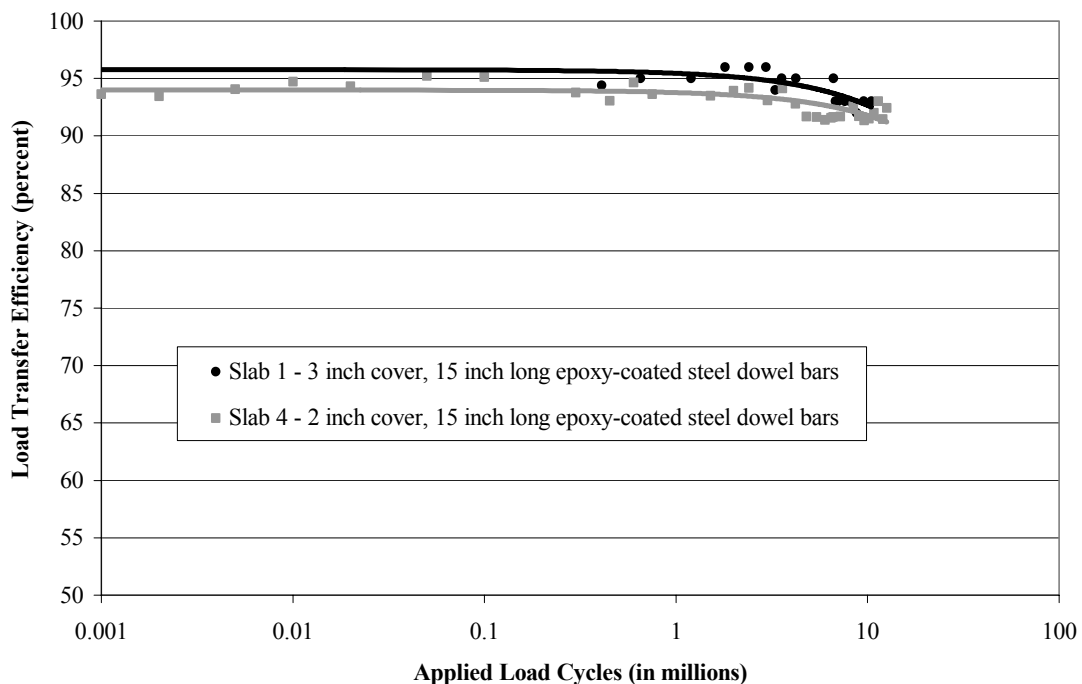


Figure 5-5 Influence of Changing Dowel Bar Configuration on Load Transfer Efficiency

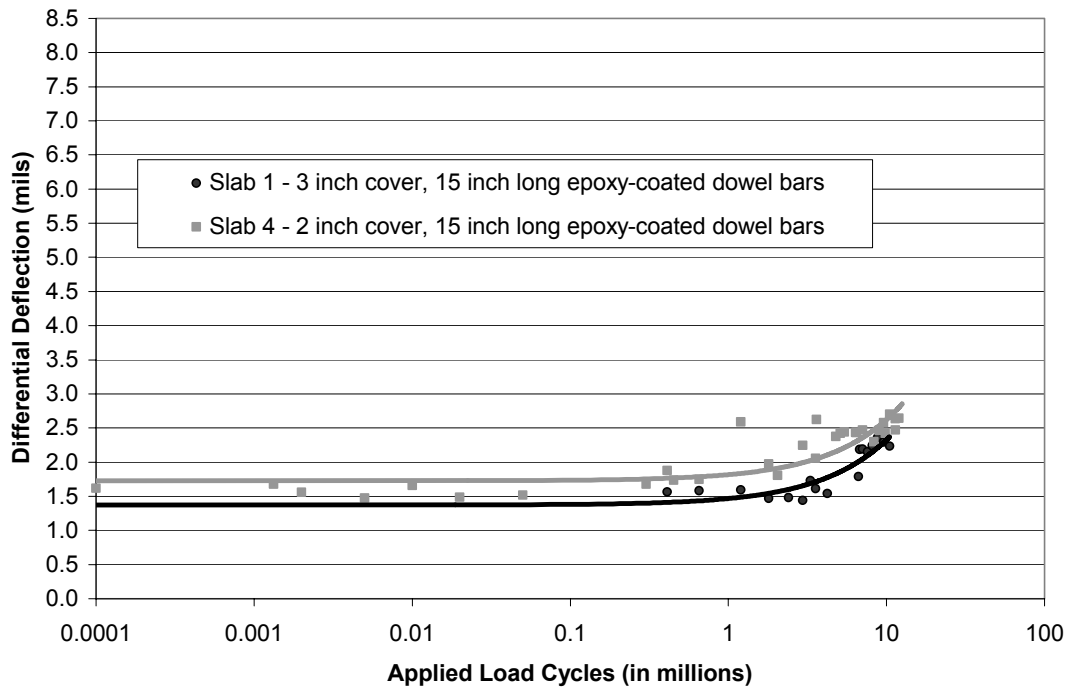


Figure 5-6 Effect of Various Dowel Bar Configurations on Differential Deflection

Slab 1, containing the dowels bars positioned at mid-depth, was again used as the control for the alternate load transfer configuration. Based on the three performance measures (LTE, differential deflection, and observed behavior), slab 4 performed at a slightly lower level than slab 1. An early decrease in performance was measured in slab 4. Slab 1 began with an LTE of approximately 95-96 percent and began to drop off slightly at roughly 6.6 million load cycles, ending with 93 percent LTE after 10.2 million load cycles. In comparison, slab 4 began with an LTE at approximately 94 - 95 percent and began to slightly drop off at roughly 2.4 million load cycles, ending at 91 percent LTE. Thus, the rate of decrease in performance was similar for both slabs, decreasing roughly 2 percent over 4 million load cycles for both test specimens. The differential deflection results were also similar, with Slab 4 having a slightly higher initial differential deflection, an earlier increase in deflection levels, and an average rate of increase of approximately 0.16 mils per million load cycles prior to termination of testing. In comparison, slab 1 exhibited an average rate of increase in differential deflection of roughly 0.11 mils per million load cycles, prior to termination of testing.

6. CONCLUSIONS AND RECOMENDATIONS

6.1 Introduction

Based on the research conducted in this project, the following conclusions and recommendations were made regarding the potential long-term field performance of three alternative dowel bar retrofit designs that addressed the issues of dowel bar corrosion and high retrofit dowel cost. In addition, it is important to note that the testing was performed in accordance with Minne-ALF test program and test procedures, and therefore was subject to the limitations of the Minne-ALF test program. This scope was limited to testing the relative performance potential of different

pavement designs using a device that mechanically loads the test specimens, simulating the repeated passage of a heavy vehicle over the test section. The testing did not account for all possible stressing factors, such as moisture and temperature gradients and changes. Due to the high cost and the long period of time required to perform the testing, only one specimen was tested for each retrofit design. It is strongly recommended that replicate testing be performed to verify these research results.

6.2 The Use of FRP Dowel Bars in Dowel Bar Retrofits

Holding all other conditions constant, the use of FRP dowel bars as an alternative to geometrically similar, epoxy-coated mild steel dowel bars in retrofit dowel bar installations resulted in lower load transfer performance. The test results show that the performance measured in the FRP doweled specimen was substantially lower than the performance measured for the epoxy-coated steel doweled specimen. This lower performance is attributed to the lower stiffness of the FRP dowels which causes an increase in differential deflection as suggested in the theoretical model developed by Timoshenko and Friberg. Although this performance difference is considerable, the performance measured in the FRP doweled specimen at the termination of testing was still above the failure criteria of 70 percent LTE and 5 mils of differential deflection. This suggests that the load transfer performance provided by FRP dowels might be adequate for field service, particularly if the lower stiffness of the FRP dowels is compensated by increasing the size of the dowels used.

It is recommended that testing be conducted on 1.75 inch and 2 inch diameter FRP dowel bars to determine the appropriate size needed to maintain a high level of load transfer. By increasing the size of the dowel bar, lower bearing stresses are developed and the stiffness of the dowel is increased, thereby improving the ability to transfer load.

6.3 The Use of Grouted Stainless Steel Dowel Bars in Dowel Bar Retrofits

The test results indicate the use of 1.66-inch diameter, 1/8-inch thick walled, 18-inch long, grouted stainless steel pipe dowel bars may perform the same as the 1.5-inch diameter, 15-inch long, epoxy-coated mild steel dowels in retrofit dowel bar installations. This conclusion is further supported by the theoretical model, which suggests that the differential deflection for the grouted stainless steel pipe dowels would be equal to that of the epoxy coated steel dowels. The test results show that the performance measured in the grouted stainless steel doweled specimen was slightly lower than the performance measured for the epoxy-coated steel doweled specimen during the first 10 million applied load cycles. After this point, the stainless steel grouted tube specimen exhibited a rapid decrease both in LTE and differential deflection. An explanation of this rapid decrease is not apparent; no visual signs of deterioration were found in the backfill material or externally on the dowel bars. An internal examination was performed on the tested dowel bars revealing that little deterioration in the grout had occurred. However, it is suggested that the type of grouted stainless steel pipe dowels tested is capable of maintaining adequate, long-term load transfer performance in the field.

It is recommended that further testing be conducted on both the grouted stainless steel pipe and epoxy coated dowel bar types to determine if the behavior exhibited after 10 million load cycles is unique to grouted stainless steel pipe dowel bar retrofits. It is also recommended that field-testing be performed to determine the effect of combined mechanical and environmental loading on the dowel bar.

6.4 The Use of Shallow Cover Retrofit Dowel Bars

The test results indicate that changing the vertical position of the dowel bars from the mid-depth of the slab to 2 inches below the riding surface in dowel bar retrofits of 7.5 inch thick PCC pavements may not reduce the level of load transfer. The test results show that the performance measured in the 2-inch cover specimen was slightly lower than the performance measured for the mid-depth doweled specimen. The rate of decline in load transfer was similar for both test specimens, but the decline began earlier in the 2-inch cover specimen. The 2-inch cover specimen was still above 90 percent LTE and had less than 3 mils of differential deflection at the termination of testing. These values are well above the failure criteria of 70 percent LTE and 5 mils of differential deflection. This information, combined with the behavior displayed throughout the duration of testing suggests that the 2-inch cover retrofit dowel bar design would be an effective way of reducing the cost associated with dowel bar retrofits.

Further testing of shallow cover retrofits, maintaining a 2 inch cover and changing the thickness of the test slab, is strongly recommended, to determine if the load transfer behavior is independent of the distance between the center of the slab to the dowel bar.

REFERENCES

1. Darter, M. I., S. H. Carpenter, M. B. Snyder, K. T. Hall, et al. Module 3H: Load Transfer Restoration. *Techniques for Pavement Rehabilitation*, Participants Notebook, Third Revision. National Highway Institute, U.S. Department of Transportation, Arlington, VA, October 1987.
2. Beer, Micheal G. *Development of an Accelerated Loading Test Platform for Pavements*. M.S. Thesis. University of Minnesota, Department of Civil Engineering, Minneapolis, 1997.
3. Mauritz, Josh A. *Design and Development of Modifications for an Accelerated Pavement Testing Facility*. M.C.E. Project. University of Minnesota, Department of Civil Engineering, Minneapolis, 1997.
4. Embacher, R. A., and M. B. Snyder. *Minne-ALF Project Overview and Retro-Fit Dowel Study Results – Development of an Accelerated Load Test Platform for Pavements*. Final Report to the Minnesota Department of Transportation. University of Minnesota Department of Civil Engineering, Minneapolis, June 1999.
5. Hall, K.T., M. I. Darter, and J. M. Armaghani. *Performance Monitoring of Joint Load Transfer Restoration*. In Transportation Research Board Record 1388, TRB, National Research Council, Washington, DC, 1993.
6. Black, Kevin N., R. M. Larson, and L. R. Staunton. “Evaluation of Stainless-Steel Pipes for Use as Dowel Bars,” *Public Roads*. vol. 52, September 1988, pp. 37-43.
7. Mn/DOT Concrete Pavement Rehabilitation Standards. St. Paul, MN, January 2000.
8. Tamms Industries. *Technical Data Sheet – Speed Crete 2028*. Tamms Industries, Kirkland, IL, May 1994.
9. MTS Systems Corporation. 790.1x Enhancements for TestWare-SX. *TestStarTM II Control Systems Manual – 150330-06A*. MTS Systems Corporation, Eden Prairie, MN, March 1997.
10. Embacher, R. A., M. B. Snyder, and T. D. Odden. “Testing of Retrofit Dowel Load Transfer Systems Using Minne-ALF,” *Transportation Research Board Record*, TRB, National Research Council, Washington, DC, 2001.
11. EDDIE, DARREN, AND SAMI H. RIZKALLA. *FIBER REINFORCED POLYMER DOWELS FOR CONCRETE PAVEMENTS*. TECHNICAL REPORT FOR ISIS CANADA, UNIVERSITY OF MANITOBA, WINNIPEG, APRIL 1999.

12. EDDIE, DARREN, AND SAMI H. RIZKALLA. "GLASS FIBER REINFORCED POLYMER DOWELS FOR CONCRETE PAVEMENTS," *ACI STRUCTURAL JOURNAL*, VOL. 98, MARCH-APRIL 2001.
 13. *HITEC EVALUATION PLAN FOR FIBER REINFORCED POLYMER COMPOSITE DOWEL BARS AND STAINLESS STEEL DOWEL BARS*. CIVIL ENGINEERING RESEARCH FOUNDATION, WASHINGTON, DC, MAY 1998.
 14. *FIBER-REINFORCED POLYMER (FRP) COMPOSITE DOWEL BARS*, MARKET DEVELOPMENT ALLIANCE OF THE SPI COMPOSITES INSTITUTE, THE SOCIETY OF THE PLASTICS INDUSTRY, WASHINGTON, DC, 1999.
 15. *GUIDE FOR DESIGN OF PAVEMENT STRUCTURES*, AMERICAN ASSOCIATION OF STATE HIGHWAY AND TRANSPORTATION OFFICIALS, WASHINGTON, DC, 1993.
-
16. Yoder, E.J. and M. W. Witczak. *Principles of Pavement Design: Second Edition*. John Wiley & Sons Inc., New York, NY, 1975.

APPENDIX A: Minne-ALF Test Frame Drawings

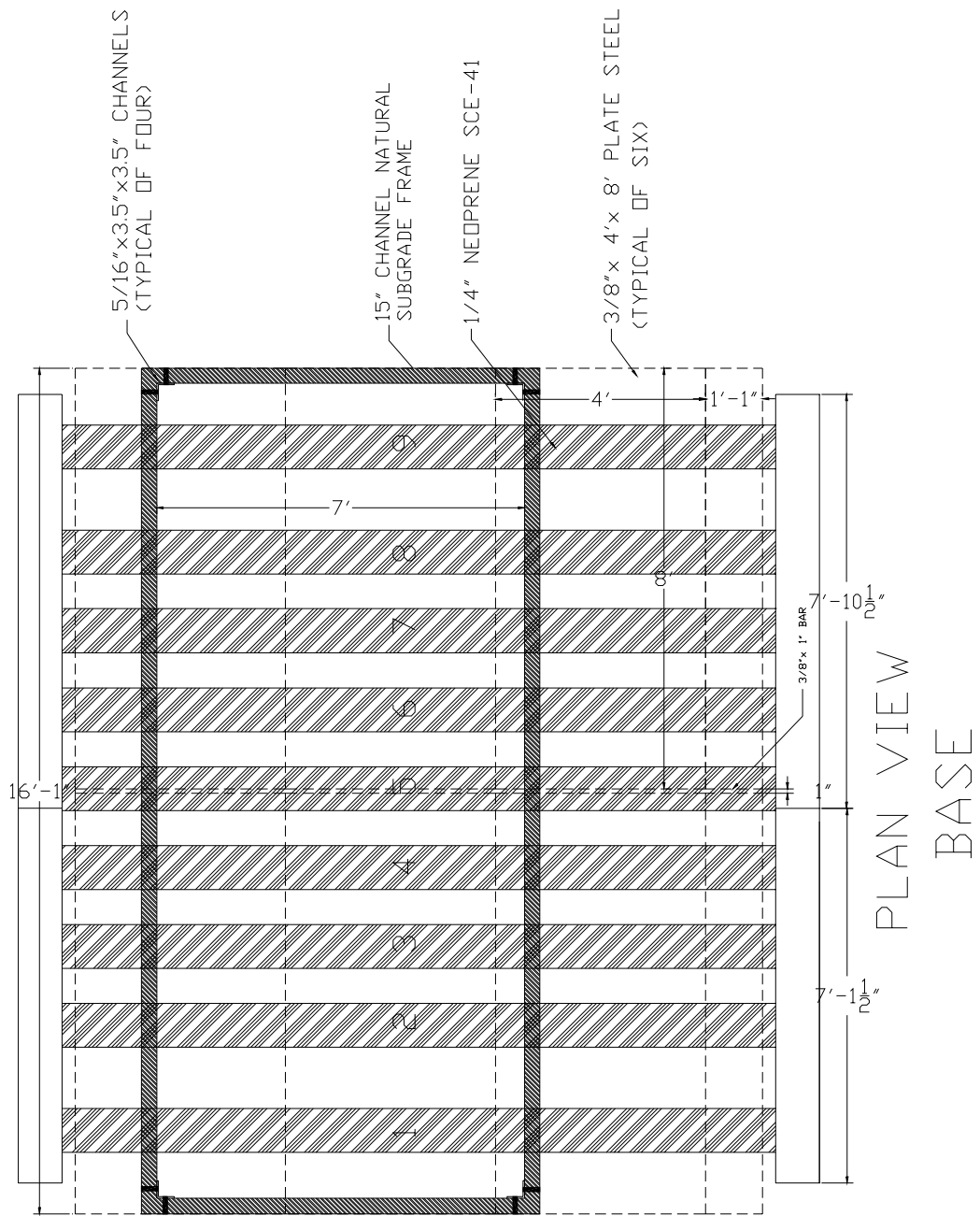


Figure A-1: Base Plan View (2)

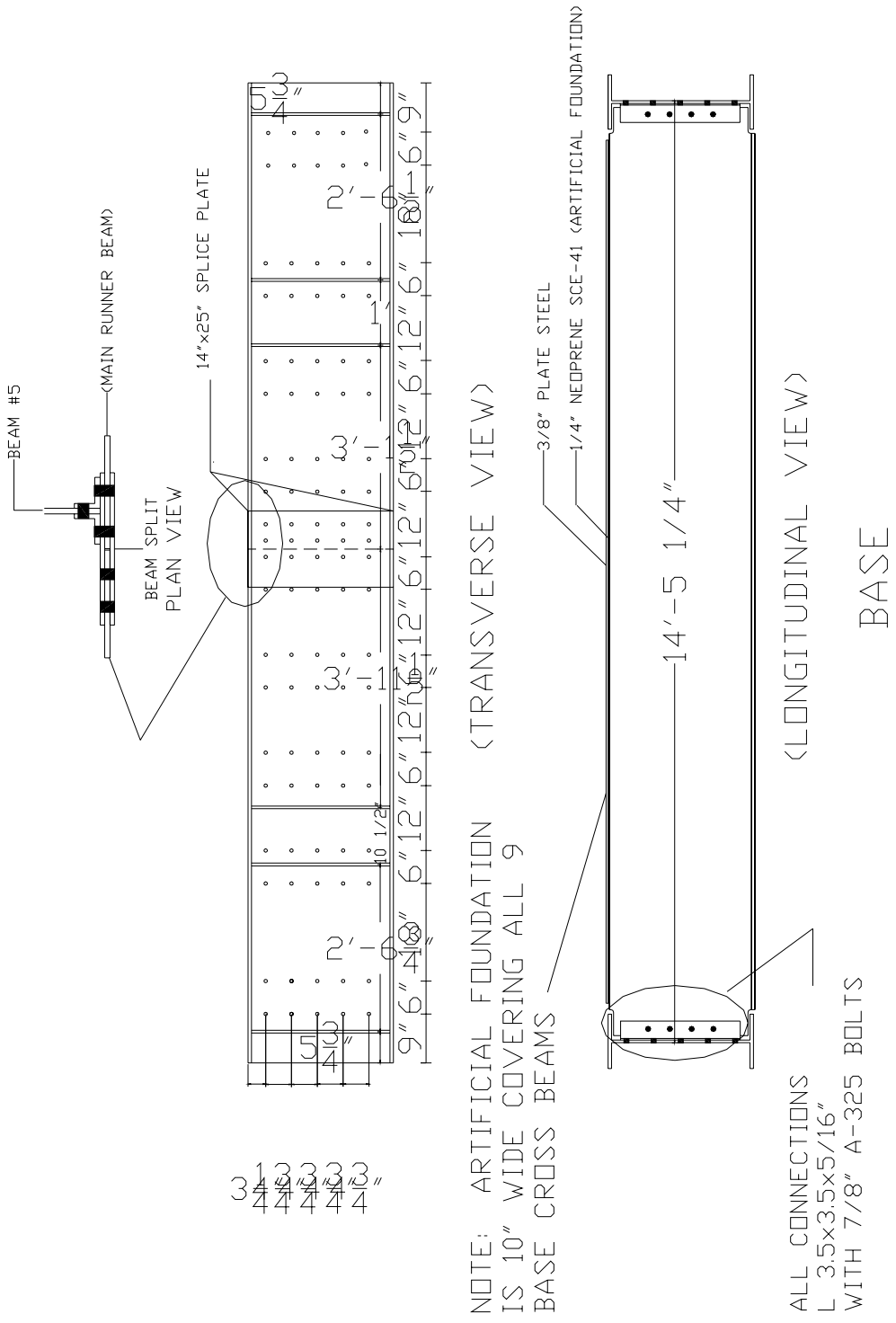


Figure A-2: Base Longitudinal View with Details (2)

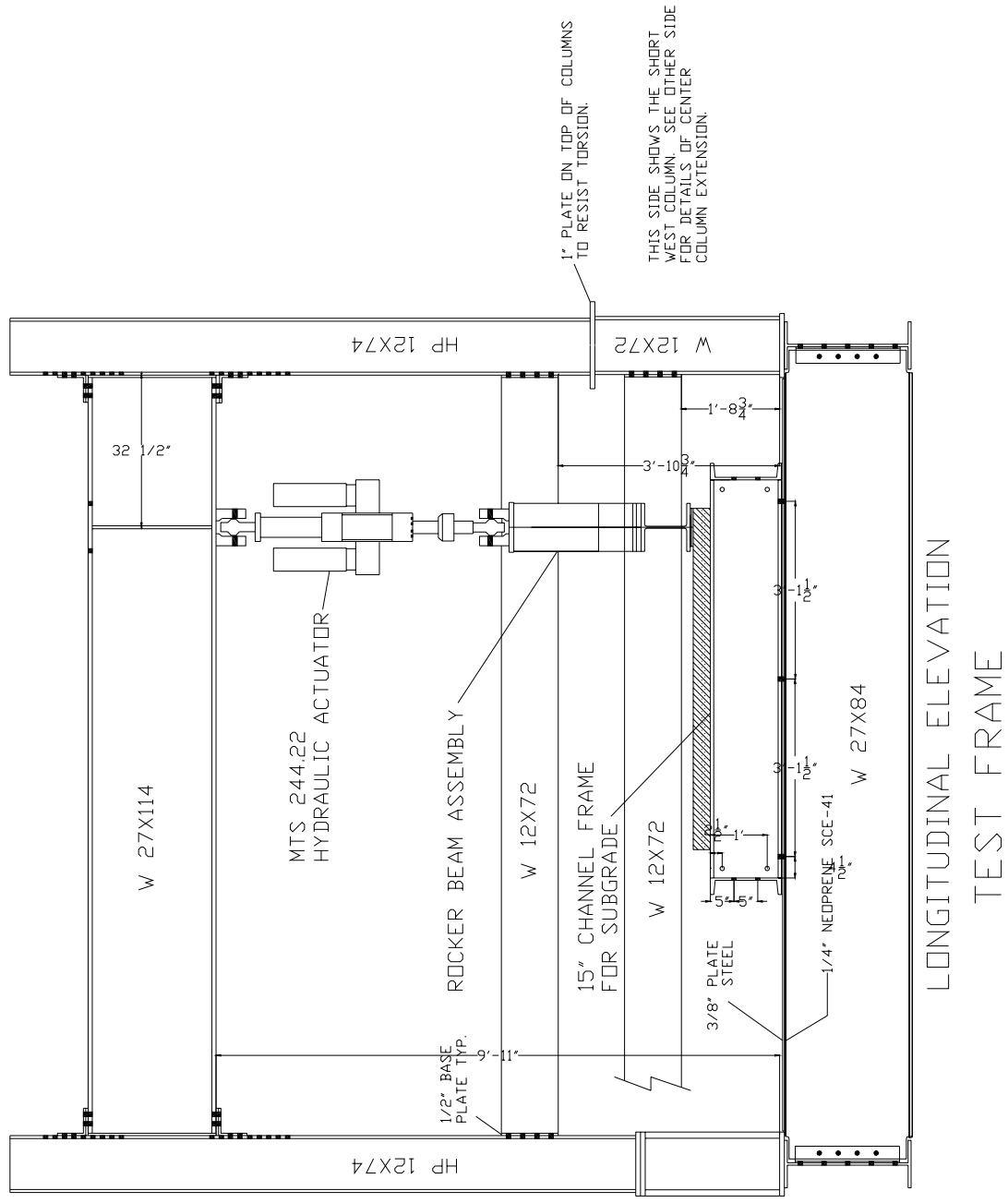


Figure A-3: Longitudinal Elevation of Minne-ALF (3)

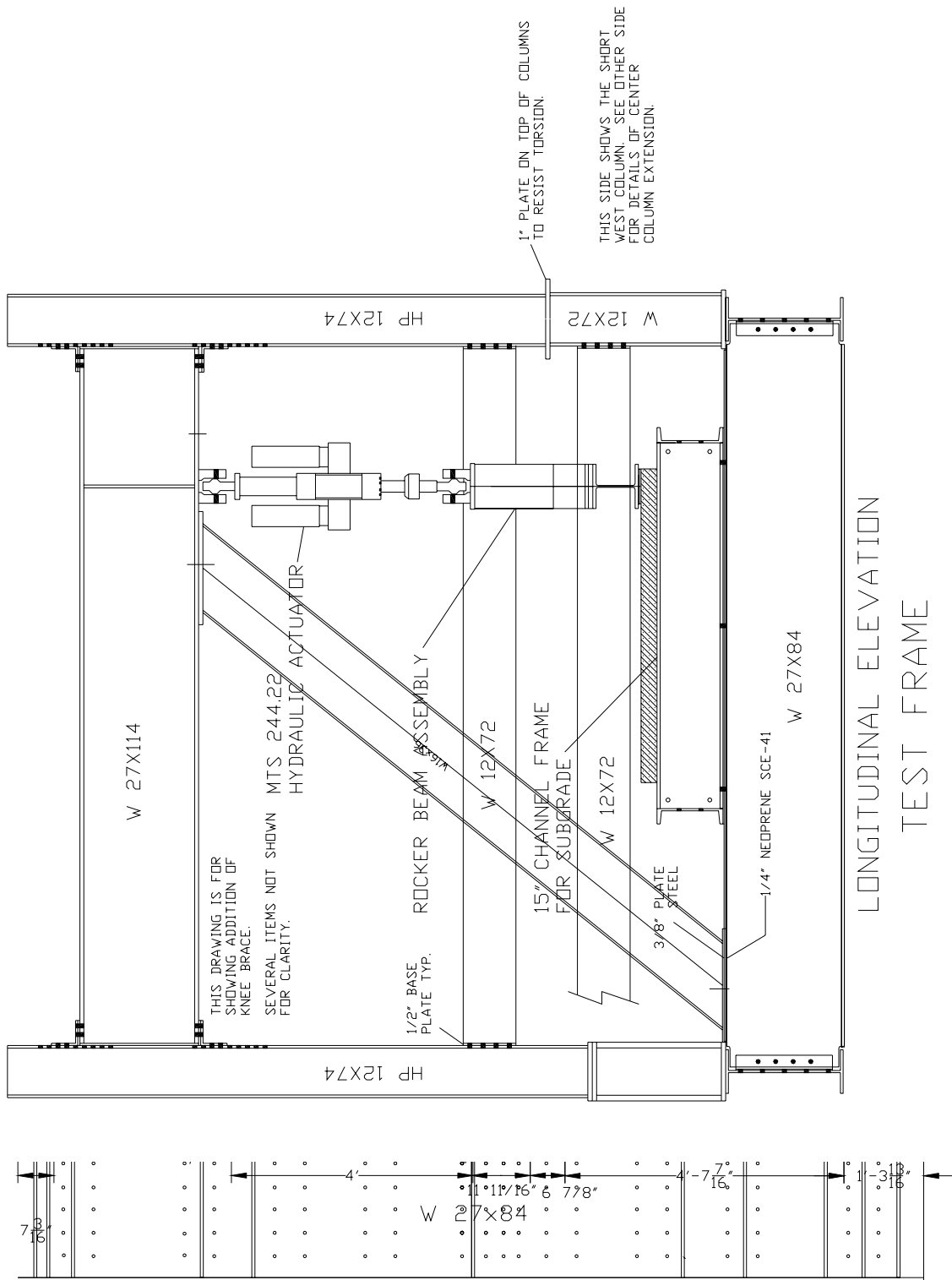
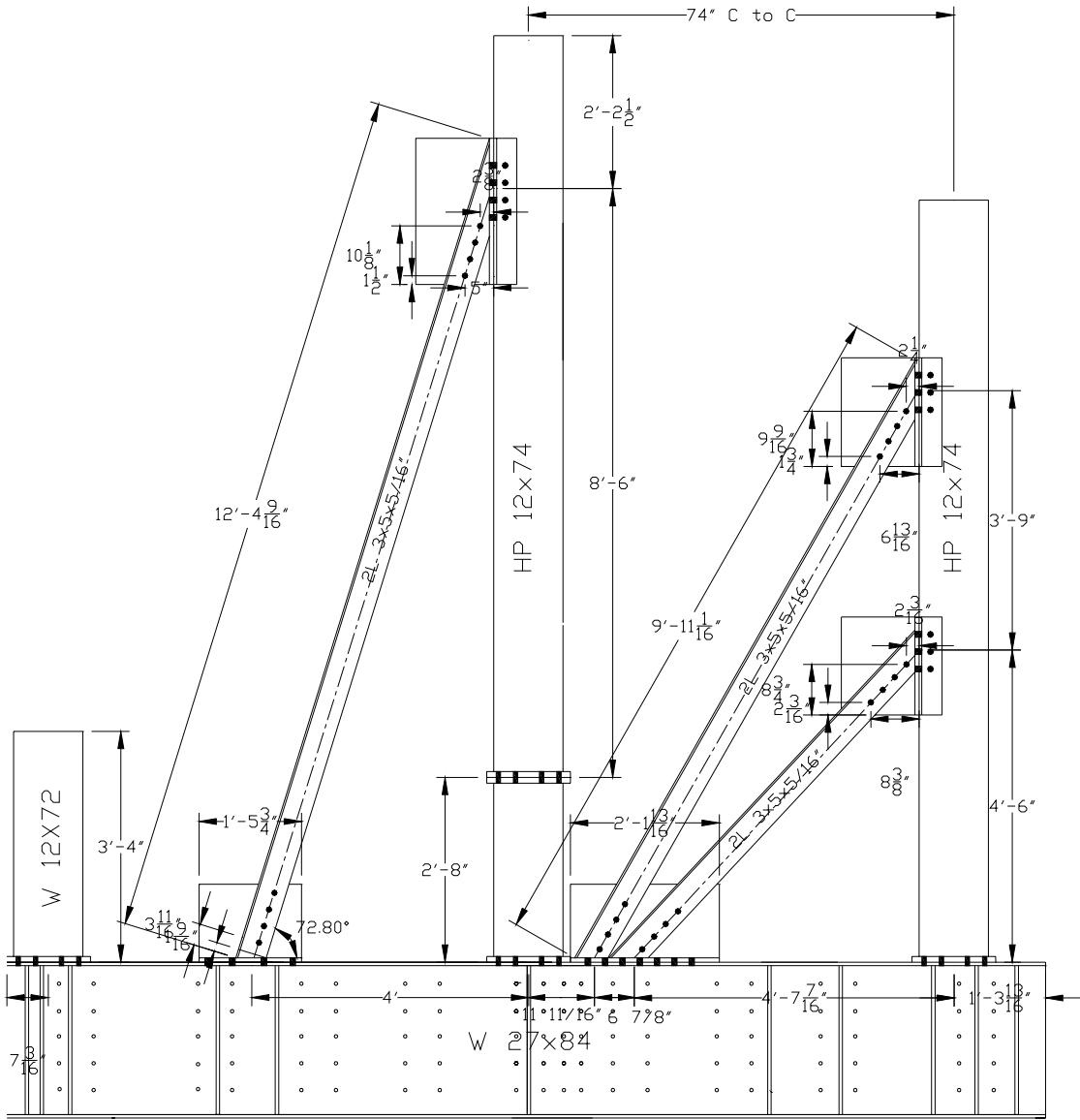
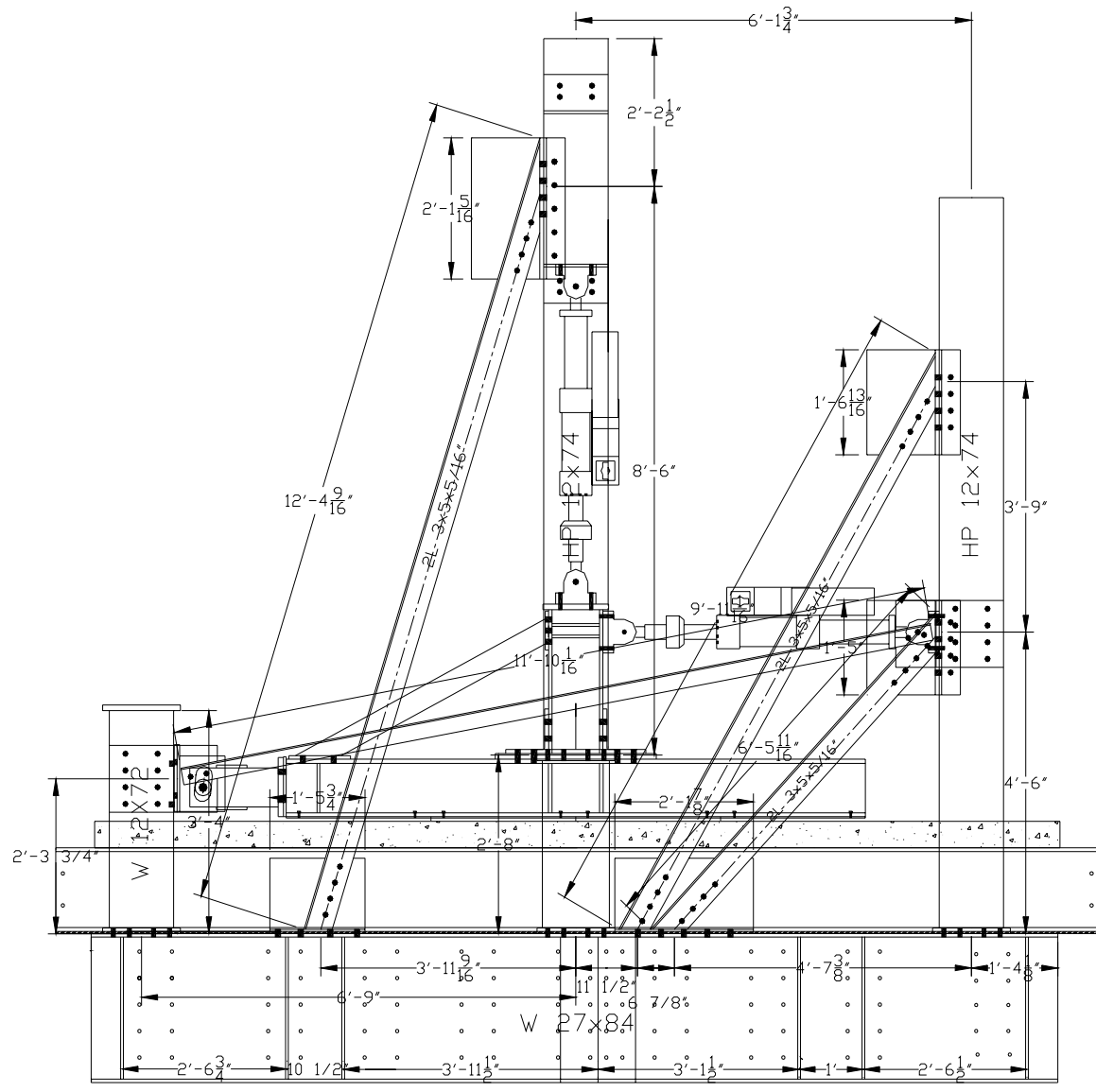


Figure A-4: Longitudinal Elevation of Minne-ALF Showing Knee Brace (3)



TRANSVERSE ELEVATION

Figure A-5: Minne-ALF Transverse Elevation (3)



TRANSVERSE ELEVATION

Figure A-6: Cutaway of Minne-ALF Transverse Elevation Showing Rocker Beam Configuration (3)

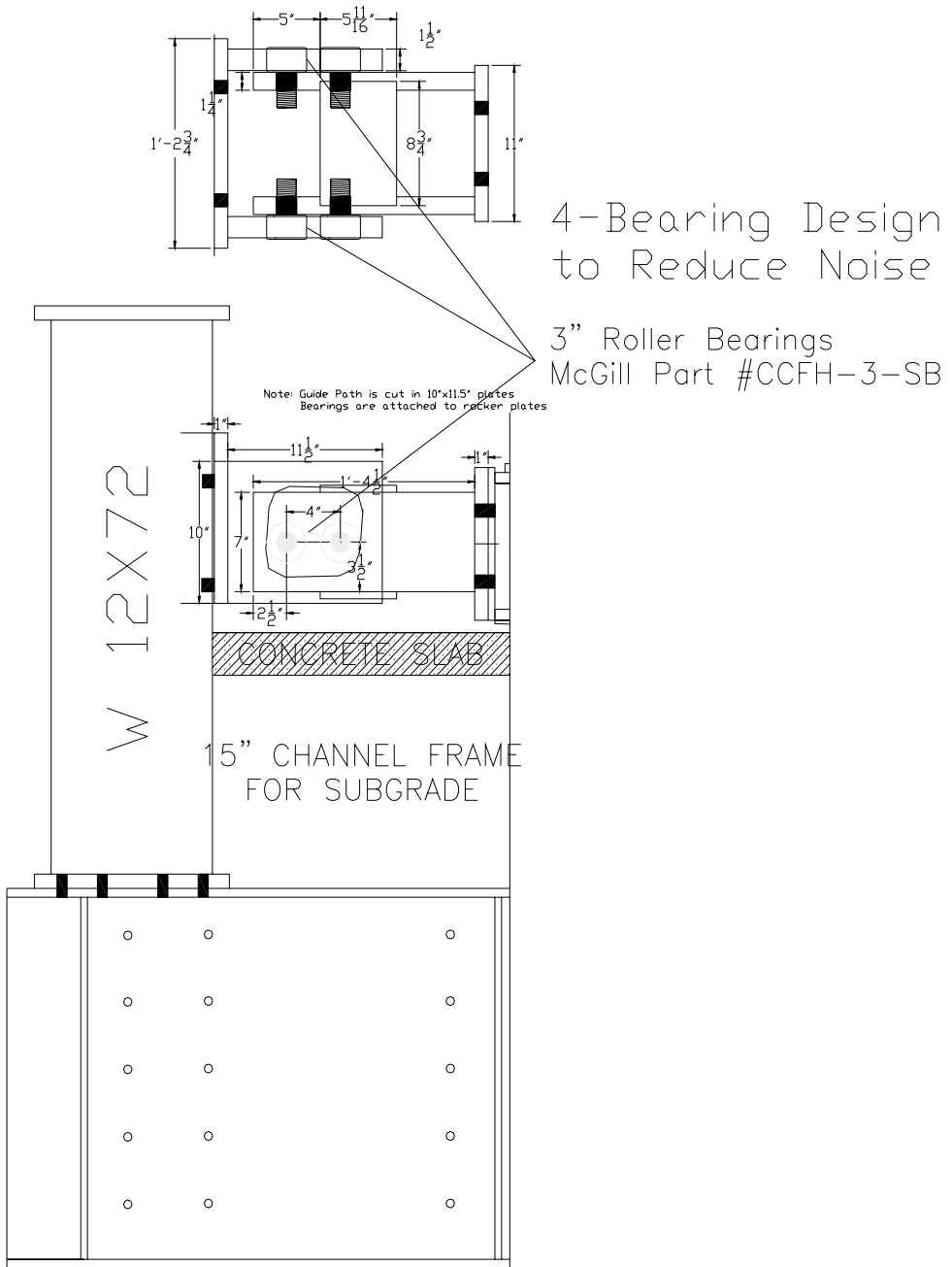


Figure A-7: Two-Pin Hinge Connection between Rocker Beam and Frame (3)

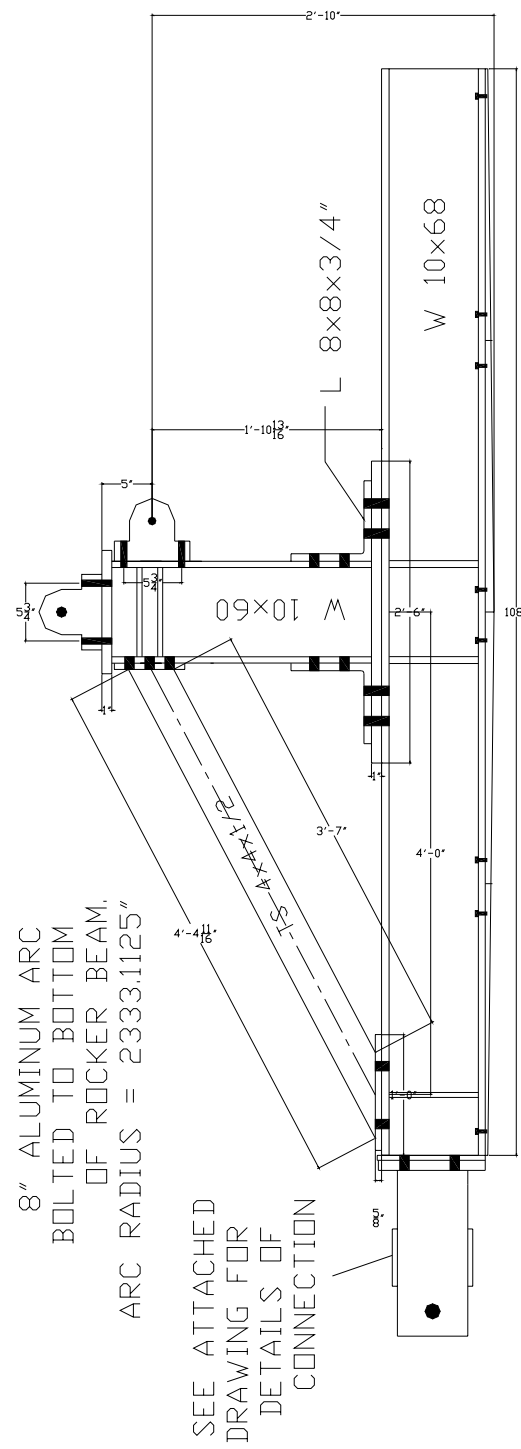


Figure A-8: Rocker Beam (3)

APPENDIX B: Minne-ALF Demonstration Testing Results

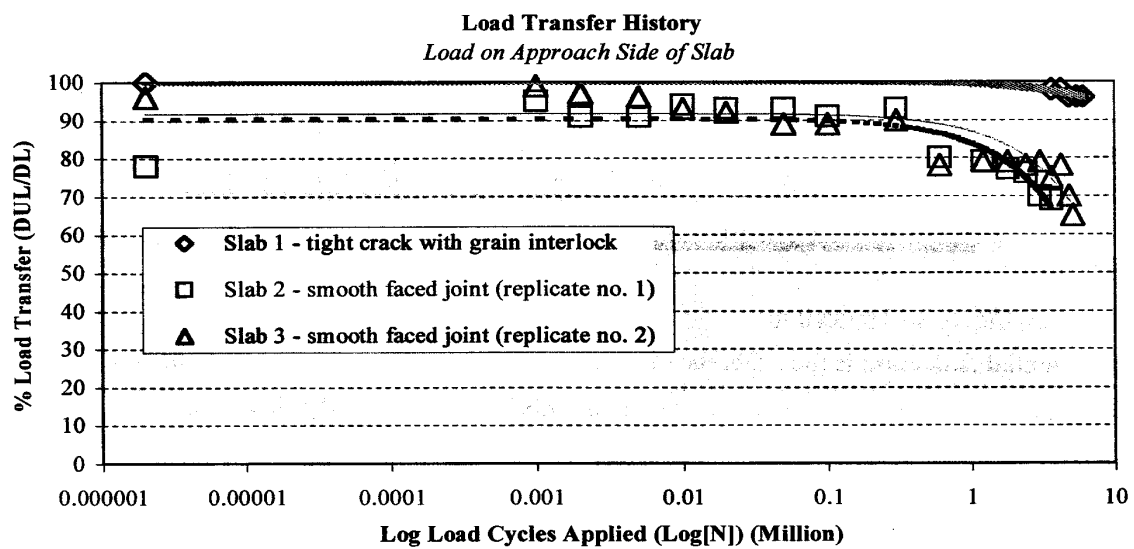


Figure B-1: Effect of Joint Face Texture on Load Transfer Efficiency (4)

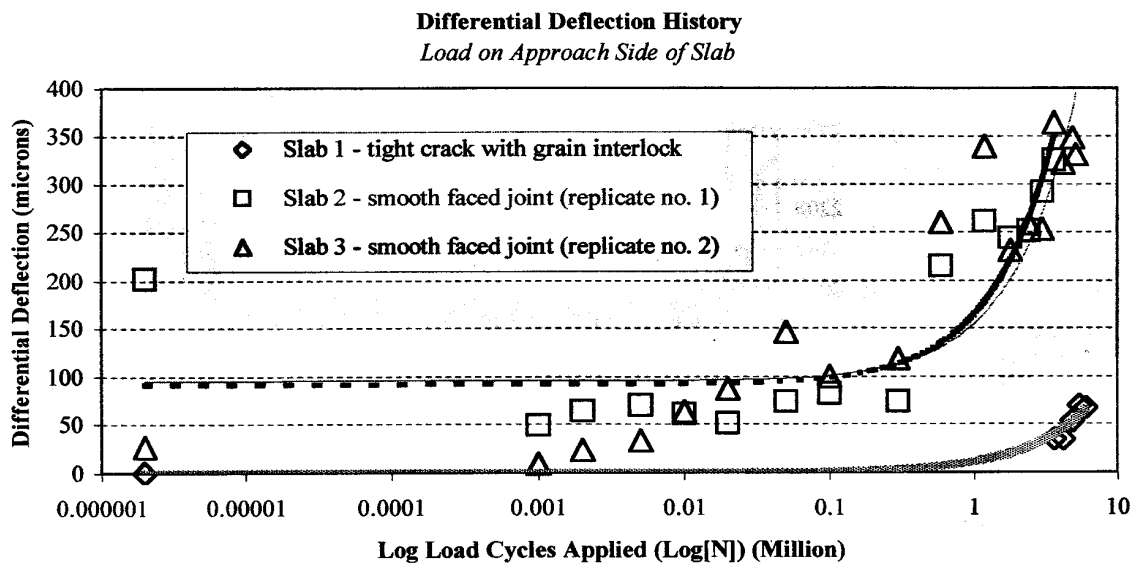


Figure B-2: Effect of Joint Face Texture on Differential Deflection (4)

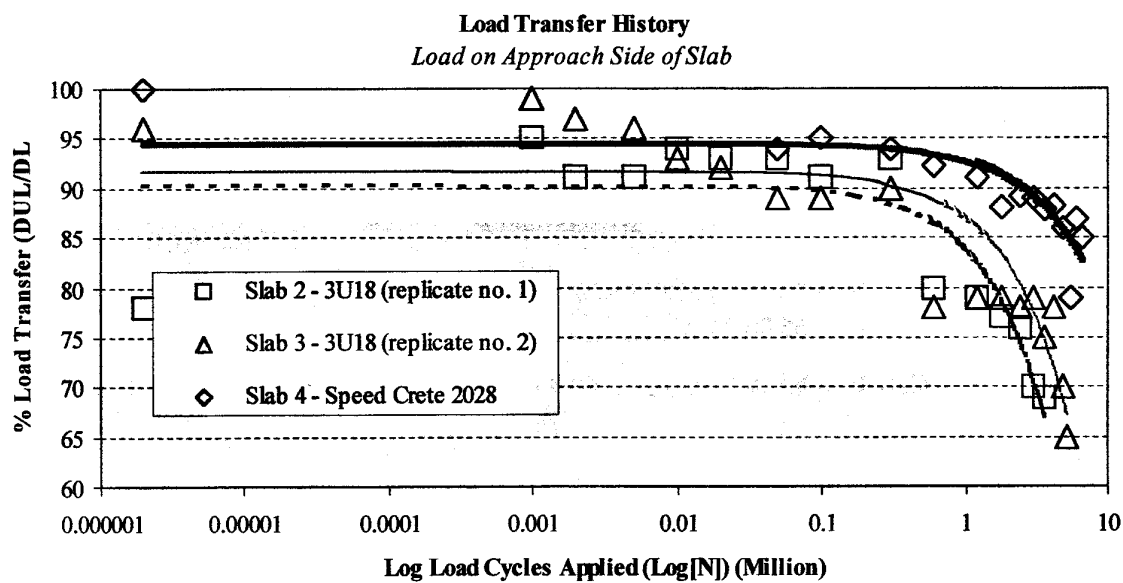


Figure B-3: Effect of Concrete Backfill Material on Load Transfer Efficiency (4)

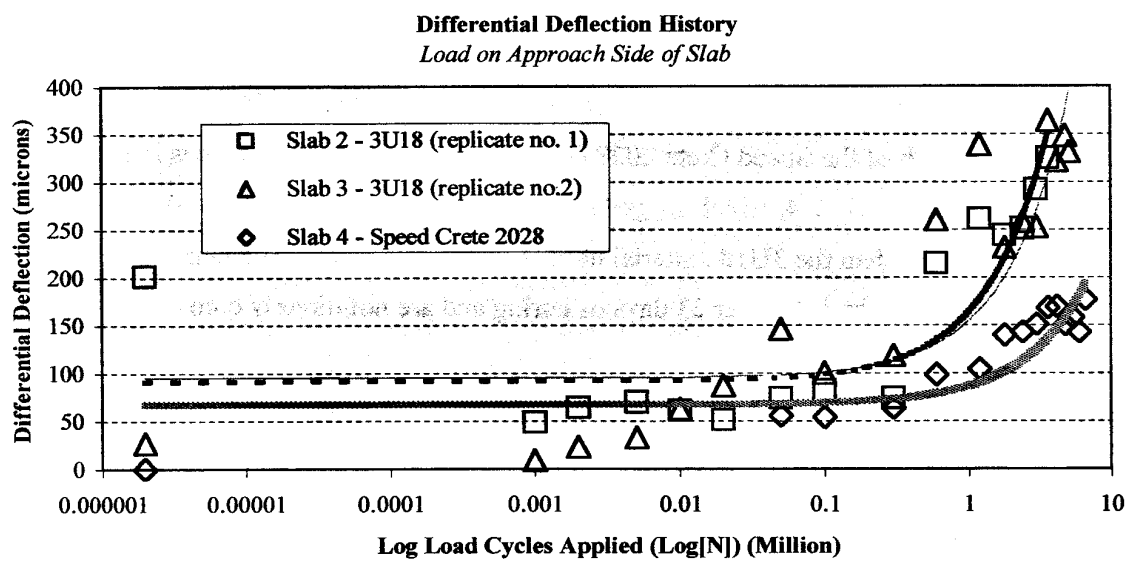


Figure B-4: Effect of Concrete Backfill Material on Differential Deflection (4)

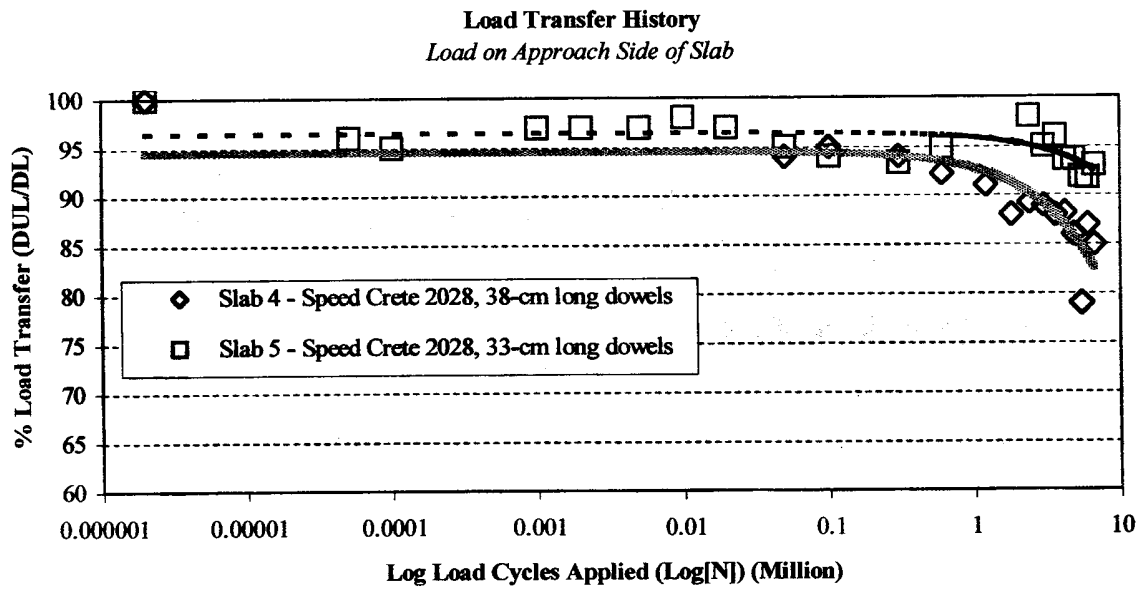


Figure B-5: Effect of Dowel Bar Length on Load Transfer Efficiency (4)

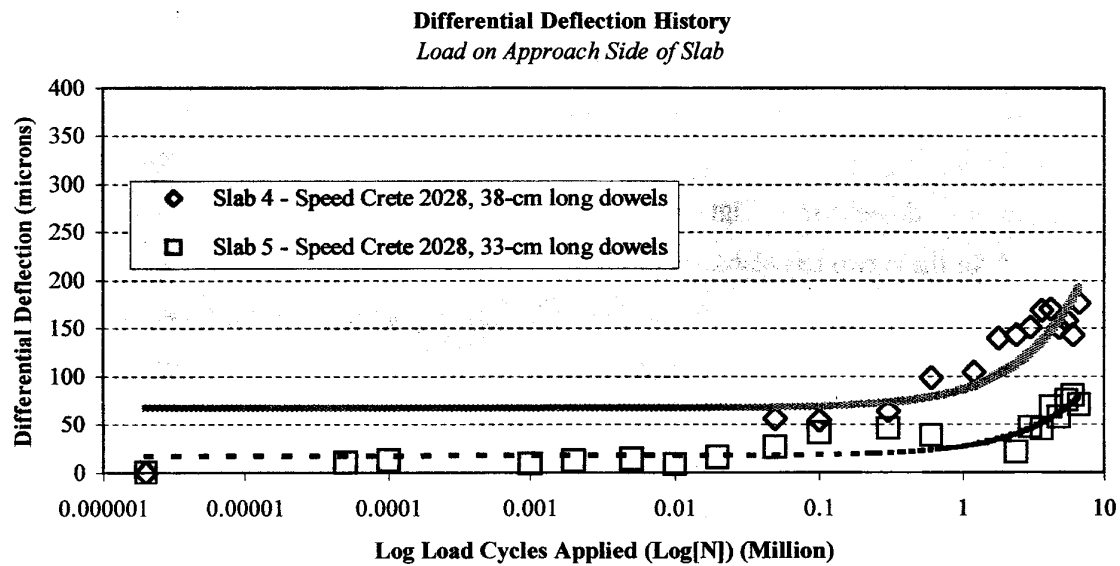


Figure B-6: Effect of Dowel Bar Length on Differential Deflection (4)

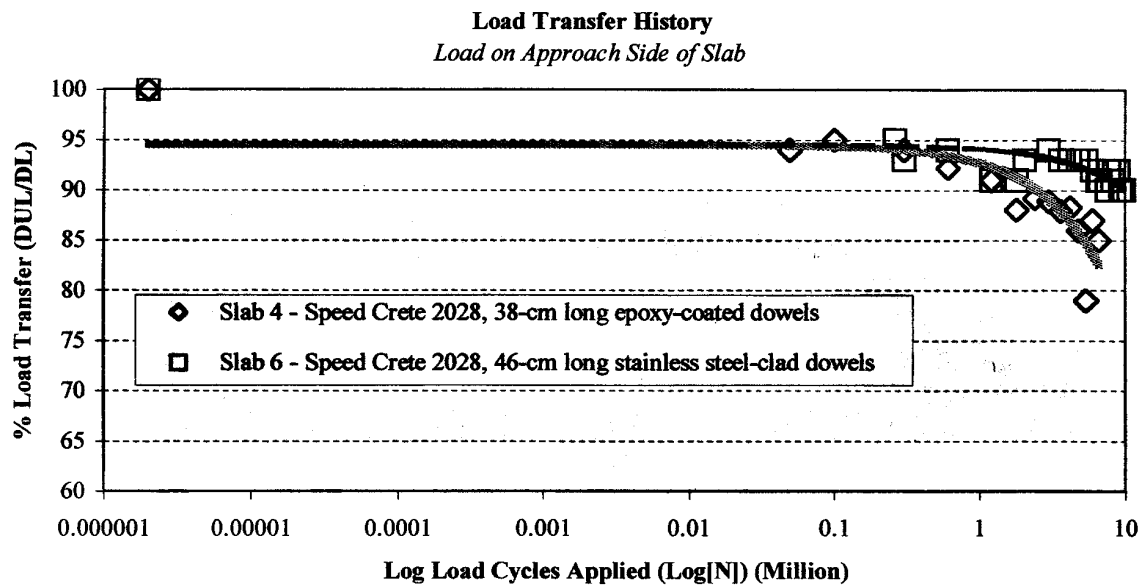


Figure B-7: Effect of Dowel Bar Type on Load Transfer Efficiency (4)

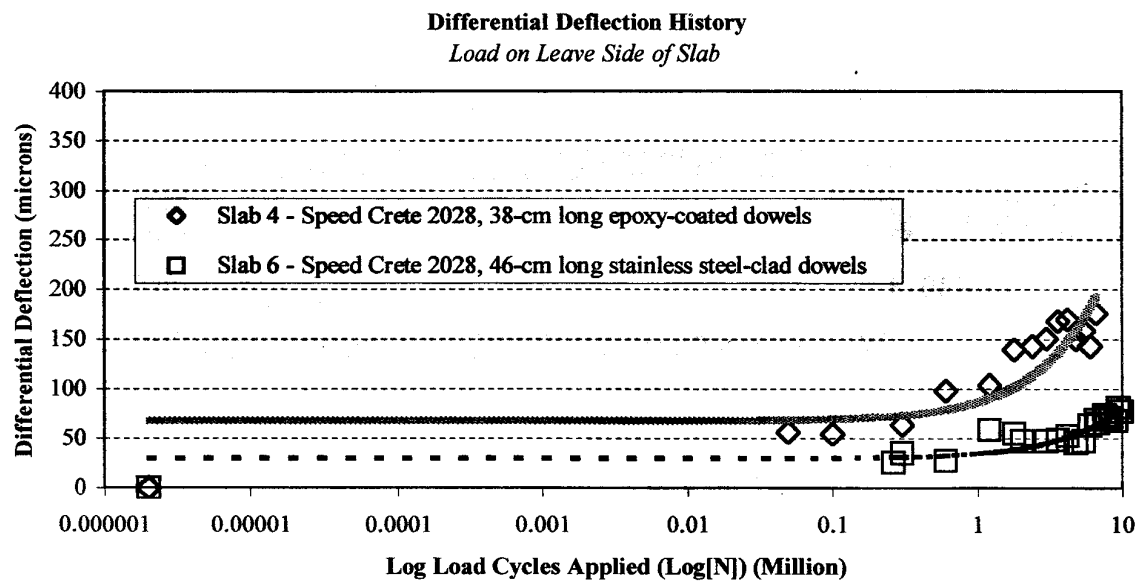


Figure B-8: Effect of Dowel Bar Type on Differential Deflection (4)